Computers and Electronics in Agriculture 158 (2019) 226–240

Contents lists available at ScienceDirect

Computers and Electronics in Agriculture

journal homepage: www.elsevier.com/locate/compag

Review

A review on weed detection using ground-based machine vision and image processing techniques

Aichen Wang[a,c,*], Wen Zhang[b], Xinhua Wei[a,c]

[a] School of Agricultural Equipment Engineering, Jiangsu University, 301 Xuefu Road, Zhenjiang 212013, Jiangsu, PR China
[b] School of Life Science and Engineering, Southwest University of Science and Technology, Mianyang 621010, Sichuan, PR China
[c] Key Laboratory of Modern Agricultural Equipment and Technology, Ministry of Education and Jiangsu Province, PR China

ARTICLE INFO

Keywords:
Weed detection
Machine vision
Image processing
Site-specific weed management
Precision agriculture

ABSTRACT

Weeds are among the major factors that could harm crop yield. With the advances in electronic and information technologies, machine vision combined with image processing techniques has become a promising tool for precise real-time weed and crop detection in the field, providing valuable sensing information for site-specific weed management. This review summarized the advances of weed detection using ground-based machine vision and image processing techniques. Concretely, the four procedures, i.e., pre-processing, segmentation, feature extraction and classification, for weed detection were presented in detail. To separate vegetation from background, different color indices and classification approaches like color index-based, threshold-based and learning-based ones, were developed. The difficulty of weed detection lies in discriminating between crops and weeds that often have similar properties. Generally, four categories of features, i.e., biological morphology, spectral features, visual textures and spatial contexts, were used for the task, which were discussed in this review. Application of conventional machine learning-based and recently developed deep learning-based approaches for weed detection were also presented. Finally, challenges and solutions provided by researchers for weed detection in the field, including occlusion and overlap of leaves, varying lighting conditions and different growth stages, were discussed.

1. Introduction

1.1. Background and motivation

With the rapidly growing global population at a rate of around 1.09% per year, the demands for more food, feed, fiber, and fuel need to be increased correspondingly, which claims higher requirements for agricultural industry to provide increasingly higher yields. The global population is expected to reach 9 billion by 2050, and agricultural production must double to meet the increasing demands (Cheng and Matson, 2015; Singh et al., 2016). However, agriculture is facing tremendous challenges including the changing climate, severe shortfall of arable land and water resources, as well as the threat from diseases, pests and weeds (Lee et al., 2010). Much effort has been exerted to weed control for decades by researchers and farmers to overcome the troublesome challenges weeds have brought. Weeds appear everywhere randomly in the field, and compete with crops for water, nutrients and sunlight, which could result in a detrimental impact on crop yields and quality if uncontrolled properly (Berge et al., 2008; Hamuda et al., 2016). Numerous studies have demonstrated a strong correlation between crop yield loss and weed competition (Hamuda et al., 2016; McCarthy et al., 2010; Slaughter et al., 2008).

In order to control weeds, different operations have been attempted, among which manual weeding by hand or using simple hand tools has been used for centuries and is still being used in small scale fields nowadays (Saber et al., 2015; Slaughter et al., 2008). However, manual weeding is too tedious, inefficient and high labor-cost, making this method not feasible for modern weeding. With the development of automation and mechanization of agriculture, mechanical weeding methods by tillage or cultivation of soil have been widely adopted for row crops and orchards (Bakhshipour et al., 2017; Nørremark et al., 2008; Tillett et al., 2008). Compared with manual weeding, mechanical methods are much more efficient and labor-saving, but they could hardly remove intra-row weeds without assistance from a target detection module, and may cause crop damage, though great efforts have been tried to design complicated mechanical hoes (Hamuda et al., 2016; Nørremark et al., 2008; Tillett et al., 2008). To achieve mechanical intra-row weeding, different assisting methods, including

* Corresponding author.
E-mail address: acwang@ujs.edu.cn (A. Wang).

https://doi.org/10.1016/j.compag.2019.02.005
Received 16 November 2018; Received in revised form 11 January 2019; Accepted 7 February 2019
Available online 14 February 2019
0168-1699/

measuring the height and diameter of crop and utilizing real-time kinematic global positioning system (RTKGPS) navigation, have been applied to locate crops and thus avoid damaging them. However, for most cases, these methods assume constant plant spacing between crops, which is unrealistic for densely sowed crops like wheat and rice. Even for transplanted and sowed crops with nominally constant spacing, there are differences between the distances of every two adjacent plants, leading to unsatisfied performance for intra-row weeding (Cordill and Grift, 2011; Nørremark et al., 2008; Tillett et al., 2008). Another widely adopted weeding method is chemical weeding, which has been the most widely used method for weed control since 1940s (Hamuda et al., 2016). Conventional chemical weeding sprays herbicides uniformly to the total field, regardless of the presence of weeds or not, resulting in high cost on herbicides. Furthermore, overuse of herbicides in agriculture has caused catastrophic environmental pollution problems (Rodrigo et al., 2014). To counteract these issues, many European countries started to restrict the use of herbicides in agriculture (Hamuda et al., 2016). Under this situation, site-specific weed management (SSWM) was introduced. The main idea of SSWM is to spray weed patches only and/or adjust herbicide applications according to weed density or weed species composition. Typically SSWM includes four processes (Fig. 1): (i) weed detection through proper sensors to provide real-time weeding information or to generate weed map for later control, (ii) decision-making to decide an action for weeding based on the previously detected information and farmer experience, (iii) execution of the weeding decision via actuator and (iv) performance evaluation of the precision operation (López-Granados, 2011). Among these four processes, weed detection plays a critical role in SSWM, since it provides essential information for the successive decision-making and implementation procedures. Precise discrimination of weed from crop benefits weed management whilst a wrongly detected weed information may fail SSWM or even cause crop damage (Haug et al., 2014).

Many different sensing methods have been attempted, including machine vision (García-Santillán and Pajares, 2018), visible and near infrared (Vis-NIR) spectroscopy (Shapira et al., 2013; Zwiggelaar, 1998), multi-/hyper-spectral imaging (Huang et al., 2016), fluorescence (Longchamps et al., 2009) and distance sensing techniques (light detection and ranging-LiDAR and ultrasonic sensing) (Andújar et al., 2013; Reiser et al., 2017). These methods can be grouped into two categories: airborne remote sensing and ground-based techniques. Airborne remote sensing commonly uses sensors mounted on balloons, airplanes, unmanned aerial vehicle (UAV) and satellites for data acquisition. The collected images are then analyzed off-line to generate weed maps for later SSWM operations. Remote sensing techniques is helpful for map-based SSWM and is well suited for large scale areas, but it is a non-real-time process and has a lower spatial resolution, compared with ground-based techniques. Ground-based sensing techniques collect and process weed information promptly and make a real-time SSWM operation possible (Lin, 2009; López-Granados, 2011). The most frequently used ground-based real-time sensors are spectrometric, optoelectronic and RGB-NIR imaging sensors. Spectrometric sensors (spectrometers) measure the reflection intensities for multiple wavelengths and provide sufficient information to discriminate vegetation from soil, but they can hardly discriminate between species, especially in early growth stages when crops and weeds have similar reflectance characteristics (López-Granados, 2011; Peteinatos et al., 2014). Though there are studies reporting using Vis-NIR spectroscopy to classify weeds from crops, they are limited to laboratorial feasibility study and rely extensively on chemometric methods to select effective wavelengths and establish calibration models (Che'Ya, 2016; Dammer et al., 2013; de Castro et al., 2012; Jurado-Expósito et al., 2003). Optoelectronic sensors measure reflection intensities within very few spectral bands, usually one or two, in the red/near-infrared (R/NIR) region. They are very prompt, efficient and cost-effective for discriminating vegetation from background (soil), and have been commercialized. WeedSeeker®, GreenSeeker® (Trimble Agriculture, Sunnyvale, CA, USA) and WEED-it (Rometron, CJ Steenderen, Netherlands) are popular vegetation sensing products on the market (Peteinatos et al., 2014; Tremblay et al., 2009). Similar with spectrometers, optoelectronic sensors could not discriminate different plants, limiting its application in SSWM. Optical imaging with machine vision technique is a very promising tool for precision agriculture and has been investigated extensively for weed detection (Saeedeh Taghadomi-Saberi, 2015). The critical procedure for precise weed detection is digital image processing, through which weed can be segmented and extracted from the acquired images. Performance of image processing is dominantly influenced by weed density, weed distribution characteristics, variable lighting conditions in the field, occlusion or overlapping of the leaves of crops and weeds, and different growth stages of plants, etc. (Lin, 2009; López-Granados, 2011; Romeo et al., 2013; Shaner and Beckie, 2014). All these factors impose difficulties to develop an efficient, uniformly robust weed sensing method. During the past decade, great progress has been achieved by researchers on overcoming these challenges and improving the weed detection efficiency and robustness. Therefore, this work was aimed at reviewing and summarizing these research advances, to provide meaningful technical information for developing more applicable and robust image processing methods for SSWM.

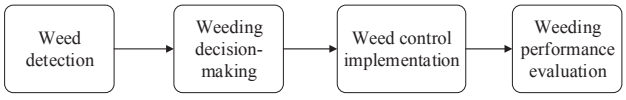

Fig. 1. Typical process of site-specific weed management.

1.2. Paper organization

This review is organized as follows: a brief overview of the workflow of image processing-based weed detection is presented in Section 2, as well as detailed discussion on the four image processing procedures for weed detection, i.e., pre-processing, segmentation, feature extraction and classification. Also presented in this section is the recently popular deep-learning based approaches for weed classification. Section 3 primarily discusses the challenges for image processing-based weed detection and possible solutions proposed by researchers during the past years. Section 4 concludes this work.

2. Overview of image processing-based weed detection

For weed detection in the field, both RGB and infrared (IR) imaging sensors have been utilized to capture field images. Then the captured images are fed as input to the processing algorithms. Typical image processing procedures include pre-processing, segmentation, feature extraction and classification (Weis and Sökefeld, 2010). Fig. 2 illustrates this general workflow and the input and output of each processing procedure.

2.1. Pre-processing

To facilitate image segmentation, original images from the camera often need to be pre-processed. General image pre-processing involves color space transformation, normalization, resizing, contrast enhancement and denoising, etc.

Regarding color space, a detailed description has been presented in the work by Cheng et al. (2001). Frequently used color space models include *RGB* (red, green, and blue), *HSI* (hue, saturation, and intensity), *HSV* (hue, saturation, and value), *Lab* (*L* for illumination, *a* for values from red to green, and *b* for values from blue to yellow), *YCrCb* (*Y* for luminance component, *Cb* for blue-difference chroma component, and *Cr* for red-difference chroma component) and so on. All these color space models can be obtained by transformation functions from RGB. Table 1 illustrates common color models and their channels, as well as the transformation functions from *RGB*. *RGB* is the most commonly

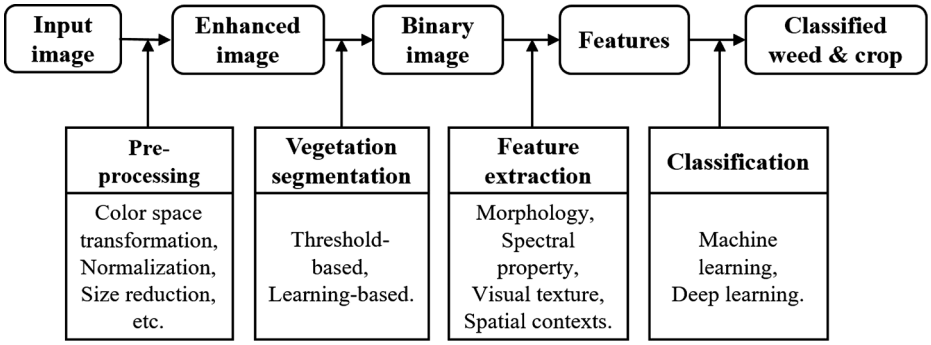

Fig. 2. General workflow of image processing-based weed detection.

Table 1
Common color models, included channels and transformation function from RGB. Channels that are used in difference spaces only appear once (García-Mateos et al., 2015).

Color model	Channel	Transformation from RGB
rgb	*R*	$r = R/(R + G + B)$
	G	$g = G/(R + G + B)$
	B	$b = B/(R + G + B)$
XYZ	*X*	$X = 0.607R + 0.174G + 0.200B$
	Y	$Y = 0.299R + 0.587G + 0.114B$
	Z	$Z = 0.066G + 1.116B$
HSV	*V*	$V = M$; with $M = \max\{R,G,B\}$; $m = \min\{R,G,B\}$; $p = 60\,m/M$
	S	$S = (M-m)/M$
	H	$H = \{p(G-B)$ if $M = R$; $120 + p(B-R)$ if $M = G$; $240 + p(R-G)$ if $M = B\}$
HLS	*L*	$L = (M + m)/2$
	S	$S = (M-m)/\min\{M + m, 2-M-m\}$
*L*a*b**	*L**	$L^* = \{116Y^{1/3}$ if $Y > k$; $903.3Y$ if $Y \le k\}$ with $k = 0.008856$
	*a**	$a^* = 500(f(X)-f(Y))$ with $f(t) = \{t^{1/3}$ if $t > k$; $7.787\,t + 0.1379$ if $t \le k\}$
	*b**	$b^* = 200(f(Y)-f(Z))$
*L*u*v**	*u**	$u^* = 13L^*(4X/(X + 15Y + 3Z)-0.197939)$
	*v**	$v^* = 13L^*(9Y/(X + 15Y + 3Z)-0.468311)$
YCrCb	*Cr*	$Cr = 0.713(R-Y) + 128$
	Cb	$Cb = 0.564(B-Y) + 128$
YUV	*U*	$U = -0.14713R-0.28886G + 0.436B$
	V	$V = 0.615R-0.51499G-0.10001B$
TSL	*T*	$T = \text{atan2}(r', g')$; $r' = r-1/3$; $g' = g-1/3$
	S	$S = [9/5(r'^2 + g'^2)]^{1/2}$
	L	$L = Y$
I1I2I3	*I1*	$I1 = 1/3(R + G + B)$
	I2	$I2 = 1/2(R-B)$
	I3	$I3 = 1/4(2G-R-B)$

used color space and is well suited for color display, but not good for segmentation and analysis, due to the high correlation among the *R*, *G* and *B* components (Cheng et al., 2001). Researchers tried to convert *RGB* to other color spaces to obtain better segmentation results. Tang et al. (2016) utilized *YCrCb* color space and *Cg* ($Cg = G - Y$) component to describe the green crops features for greenness identification under different illumination conditions, since the farmland images were mainly green components. While in the opinion of Hamuda et al. (2017), the *HSV* color space is more aligned with human color perception and robust to illumination variation. And the *S* channel correlates with the light level, which is a good choice to determine a light-dependent threshold automatically. The *HSI* and *YCrCb* color spaces were also used for greenness segmentation by researchers (Li et al., 2016; Liu et al., 2014; Sabzi et al., 2018). To meet the requirement of uniformity of color distribution, Bai et al. (2014) selected *Lab* color space for segmenting rice and cotton images with illumination variations. Similarly, Yu et al. (2018) established a Gaussian mixture model in *Lab* color space in their research to describe the distribution of crop pixel to adapt to the outdoor environment. Different color spaces were combined together to obtain more available color features. Hall et al. (2017) utilized *HSV*, *Luv*, and *Lab* color spaces to form the color feature vector [*H,S,u,v,a,b*], while Guo et al. (2013) generated 18 color features (*r, g, b; Y, Cb, Cr; H, S, L; H, S, V; CIEL*, a*, b*; CIEL*, u*, and v**) by using corresponding six color spaces. To optimize color spaces and color distribution representations for classifying soil and plant in natural, outdoors and unconstrained images, García-Mateos et al. (2015) conducted a complete and through comparison of the color spaces listed in Table 1. Results demonstrated that the *Lab* color space offered the best performance with *a** channel, producing a 99.2% of correct classification. It was concluded that the best color spaces were those could separate luminance from chrominance and channels representing a red-green axis were preferred for soil/plant classification. Later in 2016, the same research group proposed a method for selecting optimal color space for plant/soil segmentation (Hernández-Hernández et al., 2016). The proposed method was based on a non-parametric model, in which the probability density functions of plant/soil colors, $p_{plant}(color)$ and $p_{soil}(color)$, were modeled by using the normalized histogram of each class for the available training samples as shown in Eq. (1).

$$p_{class}(color) = \frac{H_{class}(f(color))}{N_{class}} \tag{1}$$

where $f(color)$ is a discretization function that maps each color to a given range, H_{class} is the histogram for a particular class and was calculated as the set of frequencies of $f(color)$ for all the training samples of that class, and N_{class} is the number of training samples available for that class (García-Mateos et al., 2015). The method was able to choose the color space that produced the best results in terms of classification accuracy for specific situation, only small amount of data needed for training. Hence, it could adapt to different kinds of objects and scenarios, and can be applied to segment multiple classes.

For images captured under insufficient illumination, noise is very likely to be introduced and the contrast of images may not be strong enough, which imposes difficulties on image processing. To remove unwanted noises, filtering methods like adaptive median filter (AMF), blur filtering, and homomorphic filtering, can be used. For images with insufficient contrast, contrast enhancement is necessary. Liu et al. (2014) enhanced the contrast of images by adjusting the grey level to the range of 0 to 255. Images captured within different wavelength bands can be fused to enhance the contrast of plants and soil (Li et al., 2013). Global histogram equalization, a standard method to normalize the histogram of images, was also adopted to enhance the contrast and alleviate lighting variations (Siddiqi and Seok-Won Lee, 2014).

Resizing of images usually refers to reducing the resolution of images and thus minimizing the computation cost. Intensity normalization or standardization is used to scale data to a reasonable scope and turn the images to normalized non-dimensional data (Tang et al., 2018).

2.2. Segmentation

For image processing, segmentation in general is defined as a process of grouping related pixels together to form connected objects that have relatively homogeneous properties (Ashok Kumar and Prema, 2013; Hamuda et al., 2016). With respect to weed detection, segmentation primarily refers to vegetation segmentation, which is a bio-class problem and the objective is to separate plants from background including soil and residues. Efficient vegetation segmentation is one of the most critical tasks for weed detection (Ashok Kumar and Prema, 2013; Sabzi et al., 2018). Tremendous research effort has been focused on the task.

2.2.1. Features for vegetation segmentation

For efficient segmentation, effective features need to be employed to discriminate between plants and background. Since plants tend to be green in color, the first feature comes to mind is color. Color is almost invariant against changes in size, orientation and partial occlusion of the object under constant lighting conditions, making it appropriate for vegetation segmentation (Bai et al., 2014). Consequently, various color-based indices, such as Normalized Difference Index (*NDI*) and Excess Green Index (*ExG*), have been put forward. Generally, these color indices can be grouped into three categories. The first category is the color indices calculated in the *RGB* color space or its normalized counterpart *rgb*. The second category is the color indices generated in other color space like *HIS*, *HSV* and *Lab*. And the third category is the indices using both of the visible and near infrared wavebands (Liu et al., 2014). Table 2 summarizes the color indices frequently used in the literature for vegetation segmentation. Most of these color indices were generated in the *RGB* color space, and can be concluded to the format of $color\ \ index = c_1R + c_2G + c_3B + k$, where c_1, c_2, c_3 and k are coefficients. Different sets of coefficients have been determined to cope with specific segmentation situations, leading to these color indices. However, none of these indices are robust enough to adapt to all segmentation scenarios. For example, the *ExG* index is easy to compute and shows good adaptability in outdoor environment, but does not perform well when the light is too high or low. Hamuda et al. (2016) summarized the advantages and disadvantages of different color indices. Apart from these indices, different color channels in different color spaces were also combined to form a color vector for vegetation segmentation. For example, Guo et al. (2013) used 18 color features (*r, g, b; Y, Cb, Cr; H, S, L; H, S, V; L*, a*, b*; L*, u*, v**) defined in 6 color spaces (*rgb, YCbCr, HSL, HSV, CIEL*a*b* and CIEL*u*v**) to extract plant from the images.

2.2.2. Segmentation approach

After feature extraction, the segmentation process will be conducted. Hamuda et al. (2016) summarized vegetation segmentation methods into three categories: color index-based segmentation, threshold-based segmentation, and learning-based segmentation. But in the opinion of the authors of this work, the color index-based segmentation is also a threshold-based method. The color index is the only feature used to distinguish plants from background. Therefore, in this review, the vegetation segmentation methods are generally grouped into two types: threshold-based and learning-based.

The concept of threshold-based segmentation is to compare the intensity values of each pixel in gray scale images with one or multiple pre-set threshold values, and then group the pixel into corresponding classes according to the comparison results (Hassanein et al., 2018; Kaur and Kaur, 2014). Gray scale images are generated by transformation with the aforementioned color indices from RGB images. The critical point of threshold-based method is to determine well suitable threshold values. A simple threshold determination method is based on empirical knowledge which produces a fixed threshold, but this fixed value is vulnerable to lighting variations and is only suited for dedicated applications (Sabzi et al., 2018). One popular automatic thresholding approach is the Otsu's method that was proposed by Otsu (1979) and has been utilized broadly. The basic idea of Otsu's method is to find a threshold that minimizes the weighted within-class variance (maximizes the between-class variance). By reviewing publications, it can be found that most vegetation segmentations are based on Otsu's method. There are also several other thresholding methods proposed in the

Table 2
Color-based indices for vegetation segmentation.

Color Index	Description	Color Space	Formulation	Reference
NDI	Normalized Difference Index	*RGB*	$NDI = 128 * \left(\left(\frac{G-R}{G+R}\right)+1\right)$	Woebbecke et al. (1993)
ExG	Excess Green Index	*rgb*	$ExG = 2g - r - b$	Guerrero et al. (2012), Saha et al. (2016), Woebbecke et al. (1995)
EG	Excessive Green	*RGB*	$EG = 2G\text{-}R\text{-}B + 127$	Chris Gliever (2001), Mathanker et al. (2010)
ExR	Excess Red Index	*RGB*	$ExR = 1.3R - G$	Meyer et al. (1999)
CIVE	Color Index of Vegetation Extraction	*RGB*	$CIVE = 0.441R - 0.811G + 0.385B + 18.78745$	Guerrero et al. (2012), Kataoka and Kaneko (2003)
ExGR	Excess Green minus Excess Red Index	*RGB*	$ExGR = ExG - ExR$	Meyer et al. (2004), Meyer and Neto (2008)
NGRDI	Normalized Green-Red Difference Index	*RGB*	$NGRDI = \frac{G-R}{G+R}$	Hunt et al. (2005)
VEG	Vegetative Index	*RGB*	$VEG = \frac{G}{R^{0.667}B^{0.333}}$	Hague et al. (2006)
MExG	Modified Excess Green Index	*RGB*	$MExG = 1.262G - 0.884R - 0.311B$	Burgos-Artizzu et al. (2011)
MExG1	Modified Excess Green Index 1	*RGB*	$MexG1 = 2G - R - B$	Ishak et al. (2009), Wu et al. (2011)
NEG	Normalized Excessive Green	*RGB*	$NEG = 2.8G - R - B$	Hong Y Jeon et al. (2011)
GMR	Green minus Green	*RGB*	$GMR = G - R$	Bakhshipour and Jafari (2018)
COM	Combined Indices	*RGB*	$COM = ExG + CIVE + ExGR + VEG$	Guijarro et al. (2011)
COM1	Combined Indices 1	*RGB*	$COM1 = 0.36ExG + 0.47CIVE + 0.17VEG$	Guerrero et al. (2012)
GPC	Green Pixel Count	*RGB*	$GPC = 2G - R * G - B$	Prema and Murugan (2016)
NDVI	Normalized Difference Vegetation Index	*RGB-NIR*	$NDVI = \frac{NIR+R}{NIR-R}$	Haug et al. (2014), Lottes et al. (2016), Philipp Lottes et al. (2016), Potena et al. (2017)
GB	g minus b	*rgb*	$GB = g - b$	Golzarian and Frick (2011), Kazmi et al. (2015)
RBI	–	*rgb*	$RBI = \frac{r-b}{r+b}$	Golzarian and Frick (2011), Kazmi et al. (2015)
ERI	–	*rgb*	$ERI = (r - g) * (r - b)$	Golzarian and Frick (2011), Kazmi et al. (2015)
EGI	–	*rgb*	$EGI = (g - r) * (g - b)$	Golzarian and Frick (2011), Kazmi et al. (2015)
EBI	–	*rgb*	$EBI = (b - g) * (b - r)$	Golzarian and Frick (2011), Kazmi et al. (2015)

Table 3
Typical morphological features for plant species discrimination.

Category	Feature	Description	Reference
Region-based shape measurement	*Perimeter*	Number of boundary pixels on segmented region in the image.	Herrera et al. (et al. (2014), Mathanker et al. (2010)
	Diameter	The diameter of a circle that circumscribes the region.	Herrera et al. (2014)
	Minor_axis_length	The length of the minor axis of the ellipse that has the same normalized second central moments as the region.	Herrera et al. (2014)
	Major_axis_length	The length of the major axis of the ellipse that has the same normalized second central moments as the region.	Herrera et al. (2014)
	Area	Number of pixels in segmented region in the image.	Herrera et al. (2014), Mathanker et al. (2010)
Region-based shape index	*Eccentricity*	*Eccentricity = Minor_axis_length/Major_axis_length*	Herrera et al. (2014)
	Form/Shape factor	*Shape factor* $= 4\pi * Area/Perimeter^2$	Ahmed et al. (2012), Lottes et al. (2016), Mathanker et al. (2010)
	Circularity	*Circularity* $= Perimeter^2/Area$	Mathanker et al. (2010)
	Compactness	*Compactness* $= Area/Perimeter^2$	Haug et al. (2014)
	Solidity	*Solidity = Area/Convex_area*, where *convex_perimeter* is the perimeter of the convex hull that contains all the plant pixels in an image.	Ahmed et al. (2012), Haug et al. (2014)
	MEC	Radius of minimum enclosing circle of the contour.	Lottes et al. (2016)
	Elongatedness	*Elongatedness* $= Area/Thickness^2$, where *thickness* is twice the number of shrinking steps needed to make an object disappear within an image.	Ahmed et al. (2012), Mursalin and Mesbah-Ul-Awal (2014)
	Convexity	*Convexity = (Convex_perimeter)/Perimeter*	Ahmed et al. (2012), Mursalin and Mesbah-Ul-Awal (2014)
	Rectangularity	*Rectangularity* = Area/(*Minor_axis_length* Major_axis_length*)	Philipp Lottes et al. (2016)
	ShapeFactor1	*ShapeFactor1 = Major_axis_length/Area*	Bakhshipour and Jafari (2018)
	ShapeFactor2	*ShapeFactor2* $= Area/Major\_axis\_length^3$	Bakhshipour and Jafari (2018)
	ShapeFactor3	*ShapeFactor3* $= 4*Area/(\pi*Major\_axis\_length*Minor\_axis\_length)$	Bakhshipour and Jafari (2018)
	rmean	The mean distance of the border to the center of gravity of an object.	Rumpf et al. (2012)
	rmax	The maximum distance of the border to the center of gravity of an object.	Rumpf et al. (2012)
	drear	Vertical distance of the border to the main axis of an object.	Rumpf et al. (2012)
Boundary-based shape descriptor	*Moment Invariants (MI)*	Functions created based on the information of both the shape boundary and its interior region. Each object is represented by a 14-dimensional feature vector, including two normalized Moment Invariants, one being the object contour and another one its solid silhouette.	Bakhshipour and Jafari (2018), Herrera et al. (2014), Ming-Kuei Hu, 1962), Pereira et al. (2012)
	Beam Angle Statistics (BAS)	A descriptor based on the beams originated from a boundary point, which are defined as lines connecting that connecting that point to the rest of the points on the boundary.	Arica and Yarman Vural (2003), Pereira et al. (2012)
	Fourier Descriptor (FD)	Fourier descriptor from an object contour is a feature vector composed of the 126 most significant coefficients of its Discrete Fourier Transform.	Pereira et al. (2012)
	Tensor Scale Descriptor (TSD)	Based on the idea that each distinct object has a shape with different distribution of the Tensor Scale orientation.	Andaló et al. (2010), Pereira et al. (2012)

literature. In the research of Guijarro et al. (2011), mean value of the gray intensity images was applied as threshold instead of Otsu's method, since they found that the Otsu's method caused under-segmentation, namely, some green pixels cannot be identified for their applications. Kapur et al. (1985) put forward a new thresholding method by using the entropy of the histogram (Tellaeche et al., 2011). Hong Y Jeon et al. (2011) determined the threshold value by dividing the pixel distribution of images to two groups by a pixel value ranging from 1 to 255. And Mursalin and Mesbah-Ul-Awal (2014) applied a local minimum threshold method to find the proper threshold value. In the method, the minimum point between two modes was used as the threshold value. Hamuda et al. (2016) conducted a comparison of different segmentation approaches in terms of their advantages and disadvantages. For details of the comparison, readers may refer to Reference (Hamuda et al., 2016). Another vegetation segmentation approach is the learning-based one. Both supervised and unsupervised machine learning algorithms have been investigated for vegetation segmentation. Reported supervised methods comprise multivariate Gaussian model (Hall et al., 2017), light weight CNN (convolutional neural networks) (Potena et al., 2017), decision tree (Guo et al., 2013), random forest (Riegler-Nurscher et al., 2018), Bayesian classifier (Tian and Slaughter, 1998; Ruiz-Ruiz et al., 2009), Back Propagation Neural Network (Zheng et al., 2009), Fisher Linear Discriminant (Zheng et al., 2010), and Support Vector Machines (Guerrero et al., 2012), etc. Unsupervised methods primarily comprise K-means clustering (Kumar and Prema, 2016; Prema and Murugan, 2016) and particle swarm optimization (PSO) based K-means clustering (Bai et al., 2014). The idea of learning-based segmentation is to learn the common properties of objects in the image by machine learning algorithms, through which pixels are classified into different categories. For supervised machine learning-based approaches, a training process is necessary to establish a classification model, and images with annotations need to be supplied as training samples. Hence, the classification model performs well for images with similar properties with the training samples, and its performance is quite dependent on the selected samples. For unsupervised approaches like K-mean clustering, no labelling is needed. Compared with threshold-based methods, learning-based segmentations are much more computation extensive and dependent on training samples, but with proper training, they can provide promising classification results.

2.2.3. Polishing segmented image

The segmented image may contain noise, mis-classified pixels and connected regions that are not desirable. Proper measures will be necessary to polish the segmented image and improve the quality. Morphological opening and closing operations are two frequently used measures to enhance the segmented image (Ahmed et al., 2012;

Bakhshipour et al., 2017; Hall et al., 2017; Herrera et al., 2014; Sabzi et al., 2018). Morphological opening is a process that applies erosion to an image firstly, followed by a dilation process, while morphological closing is a reverse process. Morphological opening has the effect of smoothing the contour of objects by breaking narrow isthmuses and eliminating thin protrusions from an image, and morphological closing is able to eliminate small holes while filling the gaps inside the contour of an image (Ahmed et al., 2012). Filtering like median filtering (Aware and Joshi, 2015; Kazmi et al., 2015) and mode filtering (Pereira et al., 2012) were also deployed to smooth the segmented images.

2.3. Feature extraction

In Section 2.2.1, features for vegetation segmentation were presented. With appropriate features and segmentation approach, vegetation (i.e., crops and weeds) could be extracted, and a mask can then be generated to remove background (soil and residue, etc.) from original images. However, crops and weeds are still mixed together which remains the most difficult task of weed detection. A variety of visual characteristics has been used to discriminate between weeds from crops and for plant species identification. These characteristics are valuable features for weed detection, which are different from those for vegetation segmentation. Generally, these features can be divided into four categories: biological morphology, spectral features, visual textures and spatial contexts (Slaughter et al., 2008; Slaughter, 2013; Weis and Sökefeld, 2010).

2.3.1. Biological morphology

For plants, biological morphology is defined as the shape and structure of a plant or any of its parts. Morphological properties, especially shape features, play an important role for identification of plant species by a human expert, thus can also be used in image analysis for weed detection (Slaughter et al., 2008; Weis and Sökefeld, 2010). A variety of shape features has been utilized for agricultural image processing and proven to be successful in distinguishing between crops and weeds, as illustrated in Table 3. Generally, shape features can be broadly categorized as features that use shape measurements and indices, and shape descriptors that are generated by transformations of segmented images (Brown and Noble, 2005). Shape measurements comprise *perimeter*, *diameter*, *minor axis length*, *major axis length* and *area,* etc.,m which are simple measurements of the segmented regions in images. Based on these measurements, different shape indices were developed by simple combinations of at least two measurements, such as *eccentricity* and *circularity*, as listed in Table 3, which belong to the category of region-based shape index. These shape indices are dimensionless numerical values, making them independent to object orientation, translation or scale (Bakhshipour and Jafari, 2018). Shape factors that are generated by transformations usually deploy boundary or contour information of segmented regions and need complicated calculations, compared with region-based shape measurements and indices. Therefore, they are often referred to region-based shape descriptors. Hu's Moment Invariants (MI) are one popular shape descriptors, which are normalized functions created based on the information of both shape boundary and interior region (Bakhshipour and Jafari, 2018; Ming-Kuei Hu, 1962). In Hu's method, each object is represented by a 14-dimensional feature vector, including two normalized Moment Invariants, one being the object contour and the other its solid silhouette. These features are independent of geometric translation, scaling, or rotation, making them to be robust to particular deformations, and could provide high discrimination ability to differentiate among objects of different classes (Bakhshipour and Jafari, 2018). The formulations for calculating MI are referred to (Ming-Kuei Hu, 1962). Fourier descriptors are a measure of shape properties of an object. It is a feature vector composed of the 126 most significant coefficients of its discrete Fourier transform (Pereira et al., 2012). Beam Angle Statistics (BAS) and Tensor Scale Descriptor (TSD) are also shape descriptors, but they are less frequently used for classification of plant species. Apart from these shape measurements, indices, and descriptors, there are other shape descriptors/features proposed by researchers. Tannouche et al. (2016) used a region-based adjacencies descriptor to discriminate between Dicot and Monocot weeds. The proposed descriptor calculated two numbers of adjacencies between a given original pixel and their adjacent pixels. The first one was the number of horizontal and vertical adjacencies, and the second one was the number of diagonal adjacencies. Applying this descriptor on all pixels belonging to one particular object, shapes with rounded and filled morphology (Dicot) and others shapes with a long and thin morphology (Monocot) were distinguished. In the research of Rumpf et al. (2012), two features derived from the skeletonisation step, which were named *skelsize* and *skelmean*, donating the length of the skeleton and the mean distance to the border of an object, were evaluated for weed species discrimination. All the shape features/descriptors illustrated above are features that fit regular discrimination scenarios. For practical applications, there are various challenges like occlusion, overlapping and damage of plant leaves, may cause less than satisfying discrimination results. To cope with these particular situations, many other features and solutions were proposed, which will be discussed in Section 3.

2.3.2. Spectral features

As discussed in Section 2.2, for image processing, spectral features, especially color indices, are valuable and effective for vegetation segmentation. For plants with different leaf colors, spectral features are effective for discrimination between them. But for plants with similar color, spectral features may result in unsatisfied performance. Some spectral features, mainly color indices, that were used for plant species discrimination are listed in Table 4. For these applications, there are obvious color difference for the plant leaves to be classified, under which condition that spectral features are effective. For example, in reference (Cheng and Matson, 2015), the Semen Euphorbia weed tended to be brown while rice plant was in green, obtaining promising classification results using only spectral features. For weeds and crops that have very similar color, using spectral features alone could hardly obtain satisfactory results. Usually other features like morphology need to be included to successfully separate weeds from crops (Ahmed et al., 2012). Compared with biological morphology, spectral features are less effective and less frequently used for plant species discrimination, but they also have their advantages. Spectral features are robust to partial occlusion and tend to be less computationally intensive (Slaughter et al., 2008). Recently, there are studies investigating the use of ground-based hyperspectral machine vision systems for plant species recognition (AlSuwaidi et al., 2016; Herrmann et al., 2013). In these studies, hyperspectral instruments were used for capturing images. In the data processing procedure, reflectance spectra were usually extracted from the hyperspectral images, and were analyzed further for plant species classification. This procedure is more about spectral analysis rather than image processing, and will not be discussed in this work.

2.3.3. Visual textures

Texture analysis is one of the most important characteristics used in identifying objects or regions of interest in an image and has been widely used in image processing for extracting useful information. Intuitively, textural features are defined as attributes representing spatial arrangement of the gray levels of pixels in a region of a digital image, which provide measures of some properties of a region such as smoothness, coarseness, and regularity (Bakhshipour et al., 2017; Bharati et al., 2004; Gonzalez and Woods, 2007). Simply, texture can be regarded as a similarity grouping in an image. Based on the methods for calculating textural features, four categories can be defined: (1) statistical features, (2) structural features, (3) model-based features and (4) transform-based features. Statistical features are calculated by analyzing the spatial distribution of gray values through computing local features at each point in an image and deriving a set of statistics from

Table 4
Spectral features for plant species discrimination in the literature.

Spectral Feature	Description	Reference
Mean Red	Average red value inside a window	Cheng and Matson (2015)
Mean Green	Average green value inside a window	
Mean Blue	Average blue value inside a window	
Std Red	Standard deviation of red inside a window	
Std Green	Standard deviation of green inside a window	
Std Blue	Standard deviation of blue inside a window	
Mean Green	Average green value in an image	Mathanker et al. (2010)
Std Green	Standard deviation of green inside an image	
Mean *r* (refer to Table 1 for *r*)	Average normalized red value of segmented object	Ahmed et al. (2012)
Mean *b* (refer to Table 1 for *b*)	Average normalized blue value of segmented object	
Std *r*	Standard deviation of normalized red of segmented object	
Std *b*	Standard deviation of normalized blue of segmented object	
NDVI	Normalized different vegetation index	Hao et al. (2015)
H	H channel in HSI color space	Li et al. (2016)
S	S channel in HIS color space	
Mean Q	Average of the 3rd component in the YIQ color space	Sabzi et al. (2018)
Additional Hue	Additional 1st component in the HSI color space	
Mean I	Average of the 3rd component in the HSI color space	
CVI_2	[ExG, GB]	Kazmi et al. (2015)
CVI_4	[ExG, CIVE, GB, ERI]	
CVI_9	[ExR, ExGR, NDI, GB, RBI, ERI, EGI, r, g]	
CVI_{14}	[ExG, CIVE, ExR, ExGR, NDI, GB, RBI, ERI, EGI, EBI, r, g, b, Gray], where$Gray = 0.2898r + 0.587g + 0.114b$	

Table 5
Statistical textural features for plant species discrimination in the literature.

Textural Feature	Description	Reference
Mean of histogram	The first moment of gray image	Cheng and Matson (2015)
Variance of histogram	The second moment of gray image	
Skewness of histogram	The third moment of gray image	
Flatness of histogram	The fourth moment of gray image	
Contrast of histogram	The intensity contrast of gray image	
Uniformity of histogram	The uniformity of gray image	
Correlation of histogram	The correlation of gray image	
Closeness of histogram	The homogeneity of gray image	
Contrast	The intensity contrast of correlation matrices	
Correlation	The correlation of correlation matrices	
Uniformity	The uniformity of correlation matrices	
Closeness	The homogeneity of correlation matrices	
Strongest	The maximum probability of correlation matrices	
Coarseness	A measure of the size of the texture elements	Prema and Murugan (2016)
Directionality	The total degree of directionality	
Roughness	Concrete variations in the texture of an image.	
Entropy	The measure of the amount of the texture information of an image.	
Line-likeness	The average coincidence of the edge directions that co-occur at pixels.	
Regularity	The degree of irregularity.	
Auto-correlation	The degree of similarity of the elements in an image.	Campos et al. (2017)
EOH	Edge orientation histogram	(Ahmad et al. (2018)

the distributions of the local features. Statistical moments of the intensity histogram of an image or region are obtained and set as statistical features like skewness, flatness and contrast of histogram. One popular approach for obtaining statistical features is the gray level co-occurrence matrix (GLCM), which was firstly introduced by Haralick et al. and yields texture characteristics such as homogeneity, contrast and the complexity of an image (Haralick et al., 1973). Table 5 lists some common statistical textural features for plant species discrimination in the literature.

Structural textures mainly refer to the composition of well-defined texture elements such as regularly spaced parallel lines. The properties and placement rules of the texture elements define the structural texture. However, structural textures are rarely used in agricultural applications since they can only describe very regular textures (Bharati et al., 2004; Materka and Strzelecki, 1998). For model-based texture, a texture image is modeled as a probability model or as a linear combination of a set of basis functions, and the coefficients of the models are used as textural features (Materka and Strzelecki, 1998; Zhang and Tan, 2002). Popular texture models include autoregressive (AR) models, Markov random fields (MRF) and fractal models. Similar with structural textures, model-based textural features are not commonly utilized for plant recognition in the literature. Some detailed discussion about

texture models can be found in references (Materka and Strzelecki, 1998; Zhang and Tan, 2002). Transformed features are extracted by transforming the images into different space whose co-ordinate system has an interpretation that is closely related to the characteristics of a texture. Frequently used transform methods are curvet and wavelet transforms (Materka and Strzelecki, 1998; Prema and Murugan, 2016). These transformations are usually conducted before the feature extraction step. The Fourier transform method is not frequently applied due to its lack of spatial localization. Various families of wavelets such as Haar and Gabor have been used for identifying some new features not easily definable in the spatial domain. Gabor filters provide means for better spatial localization and have been applied in several applications for weed and crop recognition. Chaki et al. (2015) convolved grayscale images of plant leaves with Gabor filter with experimentally determined parameters to produce a set of complex signal, which led to real and imaginary parts. After the Gabor filter procedure, GLCM was computed from the imaginary signal and a set of GLCM based features were then calculated. Similarly, Kumar and Prema (2016) and Prema and Murugan, (2016) obtained convoluted GLCM textural features from the Gabor filtered images. Compared with Gabor filter, Haar filter is more easily to conduct. In the research of Bakhshipour et al. (2017), a single-level Haar discrete wavelet decomposition was executed on the grayscale images to obtain four sub-images representing approximation image, vertical details, horizontal details, and diagonal details, respectively. Then GLCM textures were extracted from the four sub-images. Rotation-invariant wavelet features were also investigated for weed detection (Sujaritha et al., 2017). Radon transform based method is reliable for obtaining these features. It greatly reduces the number of features and quickly identifies the image at various orientations. The radon transform can reveal the impact of rotation in the input image as in the output image along θ. Then wavelet functions are used to decompose the radon output into different sub-bands, after which textural features like energy and uniformity can be calculated for each sub-band. Curvelet transformation decomposes an image at different scales and angles and benefits the feature extraction. Kumar and Prema (2016) and Prema and Murugan (2016) applied a wrapping based curvelet transform, which was a multi-scale pyramid that consisted of different orientations and positions at a low-frequency level, to the plant image to obtain the forward and backward curvelet transformation. Then angular texture pattern was extracted from the curvelet transformed image for crop and weed discrimination.

2.3.4. Spatial contexts

Plant discrimination based on morphological and spectral properties are vulnerable to variation in plant appearance that could vary distinctly within a field, between fields and during growth season, making the detecting method not robust. In contrast, the sowing pattern of crops is more stable. For most crops, they are sowed or planted in rows with prior pattern, and the spatial contexts or position information could help improve the discrimination accuracy (Midtiby et al., 2016). For cereals like barley and wheat that are sowed in row without clear distance between adjacent crop plants, the inter-row weeds can be effectively detected by identifying the centerline and edge of crop rows. All the green plants between two crop rows are regarded as weeds. Wu et al. (2011) screened inter-row weeds based on position and edge feature. The pixel histogram method was used to set centerline of crop rows, and the edge of crop row was determined with the Roberts edge detection operators. Starting from the centerline, the pixels were determined belonging to crops or weeds until the edge of crop row was reached. Liu et al. (2014) detected the inter-row weed with three main steps. Firstly, the center parts of crop row were determined with the column summation and first order derivative edge detection method. Secondly, each of the detected crop rows was connected as one region assuming that the intra-row weed, weed leaves overlapped with crops or very close to crops were very few and can be ignored. At last, the weeds were detected by comparing the area of crop rows and weeds, since each crop row was one region and the area of the region was much larger than that of weeds. It can be observed that the key procedure of detecting inter-row weeds with spatial context is to determine the crop rows and row boundaries. Various methods have been introduced for determining crop rows, among which the Hough transform are frequently used (Jones et al., 2009). Hough transform is based on computing accumulations of counts corresponding to crop rows. It was designed to deal with discontinues crop lines with missing crop plants in the crop line due to poor germination or other factors (Romeo et al., 2012). Later, Hough transform was modified to a Double Hough transform (Gée et al., 2008) and a gradient-based Random Hough transform (Ji and Qi, 2011) to improve crop row detection accuracy and computing speed. Other methods were also proposed to deal with different crop row detection scenarios including linear regression-based, blob analysis-based, alignments of green pixels, frequency analysis, stereo vision-based and vanishing point-based, etc. García-Santillán et al. (2018, 2017) and Vidović et al. (2016) proposed a global energy minimization method that used a dynamic programming technique to combine image evidence and prior knowledge about the geometric structure for crop row detection. In their approach, template matching was adopted and a series of filters was created to filter each image row. This approach worked with both straight and curved crop rows. For evaluating the performance of crop row detection method, an index named Crop Row Detection Accuracy (CRDA) was proposed. Crop row detection approach was evaluated on crops of maize, celery, potato, onion, sunflower and soybean. Results showed that the proposed approach performed better than Hough transform and one method based on linear regression, with the average CRDA value of 0.737. To improve time efficiency, Tu et al. (2014) employed a flexible quadrangle to detect crop rows. The method moved, extended or shrank a flexible quadrangle to localize crop rows in the captured frames. Experiments demonstrated that the method was effective with high time efficiency and detection accuracy. To avoid the shortcomings of Hough transform and line detection algorithms, Tang et al. (2016) mixed a vertical projection method and a linear scanning method for maize row detection. Firstly, the vertical projection method was to obtain the number and scope of maize rows, then the image bottom and top pixels were taken as two endpoints of a line. To deal with different shapes, sizes and distribution of crop and weeds when extracting rows, Burgos-Artizzu et al. (2009) developed three different methods (E1, E2 and E3). Method E1, the first and simplest one, made use of the fact that crop rows have the shape of vertical columns in images, while E2 and E3 analyzed more thoroughly the image, inspecting each image row separately via a horizontal left to right exploration. E2 regarded crop row pixels as those grouped consecutively, while E3 used border data, which was useful to point out where there were big transitions of white to black pixels. Comparison showed that each method was more accurate than the previous one, achieving better overall results, but also implying a higher computational complexity and load. Therefore, sometimes it is preferable to use E2 rather than E3, for example, when fast processing speed is required. To detect crop rows in maize images with high weed pressure, Montalvo et al. (2012) applied a method that consisted of three processes: image segmentation, double thresholding with the Otsu's method, and crop row detection. During the row detection procedure, template or mask to determine limits where pixels belonging to crop rows was built. With the template, pixels considered as outlies, probably belonging to weeds, were excluded from the estimation of parameters of the crop straight lines. This method was proved to be superior to the Hough transform method in terms of effectiveness, but required more computational operations and processing time. In 2012, Romeo et al. (2012) determined maize rows with a method based on image perspective projection that searched for maximum accumulation of segmented green pixels along straight alignments, which also overperformed the Hough transform method. For real applications in the field, there are undesired effects including vibrations, gyros or uncontrolled movements, the estimated crop rows were often less than

satisfactory compared to the real crop rows. To cope with this situation, Guerrero et al. (2017, 2013) applied a well-tested and robust Theil-Sen estimator to adjust the estimated maize rows to real ones, which improved row detection performance significantly. Most of the methods mentioned above only work with straight crop rows, while for real applications, the crop rows may be curved. In addition, uncontrolled lighting conditions in outdoor environments, defects during planting, and different crop and weed plant heights at different growth stages affect the crop row detection performance. García-Santillán et al. (2017) proposed a new method that consisted of three linked phases: (i) image segmentation, (ii) identification of starting points for determining the beginning of the crop rows and (iii) crop rows detection. For identification of starting points, the region of interest (ROI) concept with sub-ROIs and the Hough transform was applied. The ROI in the image was divided into two horizontal sub-ROIs of equal size, then Hough transform was applied to the bottom sub-ROI for identifying pixel alignments that represented the expected piecewise linear segments. Several straight lines can be determined and the intersection points between the detected straight lines with the lower edge in the sub-ROI were the starting points of crop rows. With respect to the curved and straight crop rows detection, three sequential processes were carried out: (a) extraction of candidate points through analyzing micro-ROI locations, (b) regression analysis for fitting polynomial equations (straight/quadratic) and (c) final crop rows selection and verification. Results showed that the proposed method yielded CRDA greater than 0.92 and 0.86 for straight and curved crop rows, and the processing time for one image was less than 637 ms. In a later research (García-Santillán et al., 2018), the authors used a different method for extracting candidate points for the crop rows. Rather than analyzing the locations of micro-ROI, an extra morphological dilation process was firstly applied to expand the segmented plants, after which the processed image was split into three horizontal sub-strips of equal length and a set of five points distributed along potential crop row alignments was obtained. Points one to three at the bottom of the ROI were determined by computing intersections between the corresponding reference straight line and the three horizontal lines that divided the ROI, and the remaining two point at the top of the ROI were obtained based on the idea that the row lines had the greatest accumulation of white pixels (plants). This method yielded very close results compared with the former one (García-Santillán et al., 2017).

For crops including maize, sugar beets and other high value crops that are planted in rows with a clear defined intra-row spacing between plants, it is possible to predict locations of nearby crop plants based on the prior information about plant distances within the row, thus both the inter- and intra-row weeds can be detected. Yong Chen et al. (2013) developed a stereo vision system to detect intra-row weeds when maize plants were at the early growth stages. Plants lower than 450 mm were regarded as weeds, and in the remaining plants, weeds were distinguished from maize crops by utilizing plant spacing characters, i.e., a fixed distance of 250 mm ± 25 mm. Midtiby et al. (2016) investigated the upper limit of what can be achieved by using information about sowing geometry and plant positions. The reliability of position-based crop plant detection was shown to depend on weed density and crop plant pattern position uncertainty. It was concluded that the classification based on plant position information alone was not enough for typical conditions to obtain positive predictive values of 95%. To represent the relative arrangement of sugar beets and weeds, Lottes et al. (2016) used a coordinate system that defined the crop row as x-direction and computed the difference D_i of the keypoint in x and y direction between the keypoint and all positively classified crops, based on which a plant arrangement prior feature was computed

$$p\left(\frac{w_c}{D}\right) = \frac{p(D/w_c)p(w_c)}{\sum_w p(D/w)p(w)} \quad (2)$$

where w refers to a class label, with w_c donating crops and w_w donating weeds. The class conditional probability distribution $p(D/w_c)$ and the relative frequency of the classes were learned from training data or can be provided if the information was known. Similarly, De Rainville et al. (2014) estimated the probability density functions (PDFs) for crop plants and weeds. In their research, the PDFs for the vegetation inside and outside the row were modelled by a Parzen-Rosenblatt window. Considering the rows contain both crops and weeds, while the interrows contain only weeds, the PDFs for crops and weeds were deduced, then two probabilities (weed and crop) were calculated using the Bayes' theorem and the final classification was done by choosing the higher of those two probabilities.

2.3.5. Other features

Apart from the features mentioned above, some other features were also developed for discriminating between crops and weeds. The leaves of different plant species have different vein morphological patterns, which therefore can be used for discrimination. The vein-related features were extracted by vein segmentation, central patch extraction and vein measures, and these features were used as the input of a deep convolutional neural network (CNN) for classification. Ishak et al. (2009) utilized a combination of a Gabor wavelet (GW) and gradient field distribution (GFD) techniques to extract a new set of feature vectors based on the directional texture properties for classifying weed types. GW was to enhance the directional feature of images, followed by GFD to produce histogram gradient orientation angles. A curve fitting procedure was then conducted to estimate the histogram envelope, and the curvature value of the fitted quadratic polynomial equation was extracted and used as a single input feature vector for classification. Compared with another method that used features obtained via GW only, the proposed method yielded better classification accuracy of 94%. Learning-based methods were investigated for extracting features from images. To overcome the weak generalization ability in feature extraction based on manual designed features, Tang et al. (2018) used *K*-means clustering algorithm to construct feature dictionary, which was used for feature mapping through nonlinear and convolutional approaches. The mapped features were fed to a single-layer network to construct an identification model. Hall et al. extracted the deep and abstract features with deep convolutional neural networks. A pre-trained ConvNet framework called Caffe (Hall et al., 2015) and a powerful inception architecture known as GoogLeNet (Hall et al., 2017) were used in their studies. Results confirmed the effectiveness of the deep learned features.

2.4. Classification

After extracting valuable features, different types of features are combined to improve robustness, resulting in high dimensionality of features and the "curse of dimensionality" when training models. Under this situation, feature selection or reduction is necessary to screen the most effective features and reduce the quantity. Different algorithms have been used for selecting effective features, including hybrid Artificial Neural Networks-Cultural Algorithm (ANN-CA) (Sabzi et al., 2018), Particle Swarm Optimization (PSO)-based Differential Evolution method (Prema and Murugan, 2016), quadratic discriminant analysis (Piron et al., 2008), Euclidean distance analysis (Sujaritha et al., 2017), Principal Component Analysis (PCA), Kernal Principal Component Analysis (KPCA), Linear Discriminant Analysis (LDA), Stepwise Linear Discriminant Analysis (SWLDA) (Siddiqi and Seok-Won Lee, 2014; Weis and Sökefeld, 2010) and so on.

The last step is to classify different plant varieties (crops and weeds) with proper classifiers. With different classifiers, classification between crops and weeds can be simply grouped into two categories: conventional machine learning-based classification and deep learning-based classification. Conventional machine learning-based classification generally follows the aforementioned procedures (pre-processing, segmentation, feature extraction and classification). Machine learning

refers to a group of computerized modeling approaches that can learn patterns from the data so as to make decisions automatically without programming explicit rules (Singh et al., 2016). Conventional machine learning can be grouped into unsupervised and supervised learning. Unsupervised learning starts with unlabeled data and try to find unknown patterns that enable a new, more comprehensive representation of the information contained. The most prominent task of unsupervised learning is clustering (Behmann et al., 2015). They cluster groups of similar objects that have similar features or properties without a training procedure in advance. The k-means clustering algorithm is a classical clustering approach for structuring the data based on the geometrical distribution of the data points within the feature space. It is usually used to find clustering center by minimizing the distance between the data points and the nearest neighbor center (Nasrabadi, 2007). Unsupervised learning can be used for pre- and post-processing in weed detection. Tang et al. (2018, 2017) used k-means clustering as pre-training process for unsupervised feature learning and constructing feature dictionary, while Cheng and Matson (2015) utilized a density-based spatial clustering of applications with noise (DBSCAN) as a post-processing procedure to remove the false positive weed points. The k-means algorithm was also used for filtering images and separating soil from plants (Kumar and Prema, 2016). However, the k-means approach needs to know the number of clusters, which is unrealistic for a species discriminating scenario where there can be no certainty about how many groups will be required. Under this situation, clustering algorithms, such as hierarchical clustering, diarization clustering, Dirichlet process Gaussian mixture model (DPGMM), and affinity propagation, that do not require a known number of clusters are more applicable (Hall et al., 2017). Hierarchical clustering aims to iteratively merge or split clusters based on a distance metric between clusters in order to form cluster relationship trees and allows for a more adaptable clustering system (Johnson, 1967). Diarization clustering is a variation of agglomerative hierarchical clustering where clusters are iteratively merged together based upon a relative distance metric until an ending criterion is reached. DPGMM is a form of infinite Gaussian mixture model that does not require the number of Gaussian components to be known in advance (Hall et al., 2017). And affinity propagation generates exemplars by iteratively updating how likely each point can serve as an exemplar and how likely each point could belong to each point as an exemplar (Frey and Drueck, 2006; Hall et al., 2017). Hall et al. (2017) compared these clustering algorithms for unsupervised weed scouting. It was found that hierarchical clustering yielded the best performance.

By contrast, a training procedure using labelled samples of known class is essential for supervised learning process (Singh et al., 2016). The supervised learning task consists of two phases: (1) a model (**F**) is trained by a specific supervised learning algorithm with labeled training data, and (2) The trained model (**F**) is applied to unknown data and predicts the best labels y for the test samples $\boldsymbol{X}$ by $y_i = \mathbf{F}(x_i)$ (Behmann et al., 2015). For weed detection, the labels (y_i) are 'weed' and 'crop' (or specific species of plants). Support vector machine (SVM) and artificial neural networks (ANN) are two important supervised learning algorithms that have been applied in precision agriculture, specifically, in weed detection (Behmann et al., 2015). SVM was developed based upon the theory of statistical learning. It searches for the optimal separating hyperplane that maximizes the margin between two (or more) classes and minimizes the generalization errors (Lin, 2009). SVMs contain kernel functions that are used to map samples into a higher dimensional space. The radial-basis function (RBF) kernel is a popular kernel function for both SVM training and testing operations (Bakhshipour and Jafari, 2018). ANN was inspired by the biological neural networks that constitute animal brains. In an ANN, a collection of connected units or nodes called artificial neurons were created to loosely model the neurons in a biological brain (van Gerven and Bohte, 2018). These two classifiers have been broadly applied for weed detection. SVM has been used for crop/weeds identification in maize fields (Akbarzadeh et al., 2018; Guerrero et al., 2012; Lin, 2009), weed/corn seedling recognition (Wu and Wen, 2009), weeds (*Amaranthus viridis* L., *Enhydra fluctuans* Lour., *Chenopodium album* L., *Imperata cylindrical* (L.) P. Beauv., and *Sicyos angulatus* L.) detection from a chilli field (Ahmed et al., 2012), small-grain weed species (*Cirsium arvense* and *Galium aparine*) and crops (maize, winter wheat and sugar beet) discrimination (Rumpf et al., 2012), and distinguishing broad and narrow leafed weeds (Siddiqi and Seok-Won Lee, 2014), etc. ANN were employed for robust crop and weed segmentation under uncontrolled outdoor illumination (Hong Y. Jeon et al., 2011), classification between Pigweed, Lambsquarters, hare's-ear mustard and Turnip weed (Bakhshipour et al., 2017), discrimination between 31 classes of plants (Chaki et al., 2015), and identifying three kinds of weeds (*Secale cereal* L., *Polygonum aviculare* L. and *Xanthium strumarium* L.) from potato field (Sabzi et al., 2018), etc. The performance of SVM and ANN on weed detection was also evaluated. Bakhshipour and Jafari (2018) compared the performance of SVM and ANN in detecting Pigweed, Lambsquarters, Hare's-ear mustard and Turnip weed in the sugar beet fields. SVM and ANN models was built using shape features, and results showed that SVM yielded an overall accuracy of 95.00%, slightly higher than that by ANN of 92.92%. The study of Pereira et al. (2012) on automatic classification of aquatic weeds also demonstrated better performance of SVM. Other supervised learning algorithms frequently involved in literatures include random forest (Hall et al., 2015; Lottes et al., 2016), naïve Bayesian (De Rainville et al., 2014; Mursalin and Mesbah-Ul-Awal, 2014), Bayesian classifier (García-Santillán and Pajares, 2018), AdaBoost (Ahmad et al., 2018; Mathanker et al., 2010), K-Nearest Neighbors (KNN) (Kazmi et al., 2015) and threshold-based method (Liu et al., 2014; Wu et al., 2011), etc. These are mature machine learning algorithms that find new applications in weed detection. The detailed mathematics of these algorithms will not be presented in this work. Readers who are interested can refer to corresponding publications.

Recently developed deep learning algorithms were investigated for plant classification, among which the convolutional neural network (CNN) has attracted much attention. Potena et al. (2017) exploited two different CNNs to process RGB and near infrared (NIR) images for fast and accurate crop and weed identification. A lightweight CNN was used for a fast and robust vegetation segmentation, and a deeper CNN was then used to classify the extracted pixels between crop and weed classes. The lightweight CNN, *sNet*, included a single convolutional layer with rectified linear unit (ReLU) activation function, a max pooling layer and a local response normalization step. For pixel-wise crop/weed classification, a *cNet* network was applied. The network yielded the best mean average precision of 98.7%. To detect weeds in images from winter wheat fields with heavy leaf occlusion, Dyrmann et al. (2017) trained and validated a fully CNN model that was based on the GoogLeNet architecture with a total of more than 17,000 annotations of weeds. The trained model yielded a recall of 46.3% and a precision of 86.6%, a promising result for heavy occlusion cases. In the opinion of Dyrmann et al. (2016), pre-trained networks trained on images that were very different crop/weed classification cases did not perform well. Thus, they built a new architecture that was consisted of a 5×5 convolutional layer, a 2×2 max-pooling layer, a 1×1 convolutional layer, two residual blocks, a 2×2 max-pooling layer, a 5×5 convolutional layer, a 2×2 max-pooling layer and finally two fully connected layers. The network was tested on a total of 10,413 images containing 22 weed and crop species at early growth stage. The network was able to achieve a classification accuracy of 86.2% for the 22 species. Traditional CNN uses random values to initialize the network parameters, which may lead to large errors from layer to layer propagation. To solve this problem, Tang et al. (2017) set k-means unsupervised feature learning as a pre-training process, and replaced the random initialization weights of traditional CNN parameters. This method gained higher weed identification accuracy, with 92.89% accuracy, beyond 1.82% than CNN with random initialization and 6.01% than the two layer network without fine-tuning. These trained CNN

models could yield very promising weed detection accuracy, but with large amount of parameters and heavy computation load, making them unsuitable for on-line applications. To reduce the number of parameters and speed up the processing procedure, McCool et al. (2017) proposed a novel approach for training CNNs. The approach consisted of three stages: (i) adapt a pre-trained model (Inception-v3) to provide state-of-the-art performance, (ii) employ *teacher-student* network to compress the models and learn a lightweight CNN that was less accurate but had two orders of magnitude fewer parameters, and (iii) combine multiple lightweight models as a mixture model to enhance the performance. The combined lightweight models achieved accuracy greater than 90%, with processing speed between 1.07 and 1.83 frames per second, while using considerably fewer parameters. To further reduce the processing time, Milioto et al. (2018) combined existing vegetation indexes and a CNN network, with the vegetation indexes as the inputs of the network. The network was an end-to-end encoder-decoder semantic segmentation network with convolutional layer, pooling layer, residual separable bottleneck, pooling indexes, encoded feature volume and unpooling layer. The method operated at round 20 Hz, which is suitable for online classification in the fields. Furthermore, the proposed approach could act as a robust feature extractor for images not represented in the training set, requiring little data to adapt to new environment.

3. Challenges and possible solutions

For ideal image capturing environment and specific plant growth stage, the current image processing techniques provide very promising classification results. However, for real applications in the field, the task becomes extremely challenging. The leaves of crops and weeds often overlap over each other at late growth stages, making them indistinguishable from each other. Sometimes the plant leaves are occluded or damaged by unwanted material including clays and dead leaves, changing the morphological and spectral properties of leaves. The varying lighting conditions, the shadows of plant canopy and the solar angle can directly impact the vegetation color (Bai et al., 2014). Last but not least, different growth stages of plants also change the morphological, textural and spectral properties of leaves (Shaner and Beckie, 2014). Research regarding addressing these challenges is discussed in this section.

Occlusion and overlap of plant leaves often occur at late growth stages (Fernández-Quintanilla et al., 2018). Under this situation, morphological features may not perform well since the shape of leaves is changed unpredictably, and the overlapped leaves tend to be segmented as one object. The active shape models used by Søgaard (2005) only deal with young weed seedlings with up to two true leaves and without mutual overlapping with other leaves. In 2008, the active shape models were constructed using different training images and different description levels with 19%-53% occluded crops (Persson and Åstrand, 2008). With proper training data set, up to 83% of the occluding weed can be removed. Dyrmann et al. (2017) trained a fully CNN based on GoogLeNet architecture to detect weed locations in leaf occluded cereal crops, which yielded a recall of 46.3% and a precision of 86.6%. But these methods lack of generality, limited to specific training data set. Rather than processing the whole image, Ahmad et al. (2018) extracted local shape features by dividing the entire image into d × d sub-images, to alleviate the effect of overlapping. But for heavy overlapping scenarios, the performance was still unsatisfactory. Another similar approach, keypoint-based approach, was applied by Lottes et al. (2016) and Philipp Lottes et al. (2016a). The authors computed features and performed classification for each pre-defined keypoint individually in the image. Results demonstrated that this method could deal with plants that overlap but at the cost of being computationally expensive. To balance the classification accuracy and speed, they combined the keypoint-based and object-based approaches. Initially the object-based approach was applied to the whole image to identify objects as weeds or crops. For uncertain objects, the keypoint-based approach was applied to improve the classification accuracy. The idea of keypoint-based classification was also adopted by Haug et al. (2014). The classification results obtained at the keypoints were spatially smoothed using a Markov Random Field and continuous crop/weed regions were inferred in full image resolution through interpolation to further improve the performance. The method generally handled field situations with and without overlap with an average classification accuracy of 93.8%. Plant height helps to solve the occlusion and overlap problem as weeds and crops often grow at different speeds. Piron et al. (2010) extracted plant height information using an active stereoscopy technique, based on a time multiplexing coded structured light developed to deal with occlusion and thin objects. The light was coded binarily and projected onto the plants via a video projector. After image caption, the distance between plant pixels and the actual ground level was computed as a corrected plant height. Overall classification accuracy reached 83% by using the corrected plant height for cases with the presence of numerous occlusions.

Another challenge is the varying lighting conditions in outdoor environment. Different illumination conditions lead to different colors, noise levels, shadows, reflection, contrast, saturation and brightness of the same scene, further result in failure of the segmentation/classification algorithms, especially those threshold-based ones. To improve the performance of algorithms under variable lighting conditions, different color space models have been used. Tang et al. (2016) stated that the *YCrCb* color space model was very suitable for processing images sensitive to illumination changes since the luminance and chrominance are separated in this model. But the *YCrCb* color space model lacked the differences between green signal and light brightness, so the authors adopted the Cg component, which was translated from the *RGB* color space, to describe the green crop features. In the research of Hamuda et al. (2018, 2017) and Yang et al. (2015), the *HSV* color space was used for greenness identification and image segmentation under natural illumination (cloudy, partially cloudy, and sunny). Other color space models were also investigated and recommended, including *L*a*b** (Bai et al., 2014), *RGB* (Guo et al., 2013), *rgb* (Tian and Slaughter, 1998), *HSI* (Zheng et al., 2009), Hue-saturation (*HS*) and hue (*H*) (Ruiz-Ruiz et al., 2009). However, it seems that the recommended color space models differ depending on target plants, and none is universal. Apart from selecting proper color space model, different processing methods were proposed to alleviate the effect of varying illuminations. Siddiqi and Seok-Won Lee (2014) exploited the usage of global histogram equalization in the pre-processing stage to minimize the effect of lighting by lengthening the intensity of dynamic range using histogram of the whole image. Guo et al. (2013) trained a decision tree model with series of images taken automatically regardless of lighting conditions for vegetation segmentation. After segmentation using the trained model, noise reduction filters were adopted to polish the segmented images. Results showed that the decision tree-based method outperformed those based on *ExG, ExG-ExR* and *MExG*, under various natural lighting conditions. The shortcoming of this method was that it depended too much on the training dataset. To address the weak contrast and high saturation caused by illumination, Romeo et al. (2013) designed an expert system for greenness identification, which consisted of two main modules: (i) decision making by histogram analysis to analyze the quality of the incoming image; (ii) greenness identification with two different strategies. For images with sufficient contrast, the index *COM* combined with Ostu method was used for segmentation, while for those with insufficient contrast, image preprocessing by down-sampling and smoothing, and fuzzy clustering with dynamic threshold was employed for segmentation. The method gave percentage of correct classification of 0.95 for different images captured with several camera devices. Yu et al. (2018) introduced a Gaussian mixture model in *LAB* color space to describe the distribution of crop pixels to adapt to outdoor environment, after which super-pixel technique was used to segment the image into numbers of sub-areas. To enhance the crop detection performance in sunny conditions, Kalman filtering was

applied to predict the new position of cauliflower plant in video sequences, and the Hungarian algorithm was used to assign each detected crop to correct trajectory. In sunny conditions, overall detection performance raised from 97.29% to 99.34% (Hamuda et al., 2018). Ahmad et al. (2018) found that the optical threshold value for segmentation could be computed for each image dynamically using the mean intensity value of the image being observed to minimize the effect of illumination, which was named adaptive segmentation and proved to be effective. Instead of improving the image processing algorithm alone, another idea to alleviate lighting effect is to improve the image quality when acquiring images. Sujaritha et al. (2017) fixed a special light ring (Magideal Luxury Selfie Luminous LED Light Up Phone Ring) at the camera to avoid the interference of shadows and other illumination related obstacles, thus improving the image quality.

Different growth stages of plants change morphological, textural and spectral properties of leaves, reducing performance of classification models. This remains a big challenge and few research was focused on solving this issue. One general and commonly adopted approach is to train the classification model with samples of different growth stages (Hassanein et al., 2018; Hong Y. Jeon et al., 2011; Rumpf et al., 2012). This approach is straightforward and simple, but compromises on classification accuracy and often needs large amount of samples. Another similar concept is to retrain the classification model with new samples when its accuracy is unacceptable. This method produces higher accuracy, but the retraining process is tedious and time-consuming. Lottes et al. (2018) developed a sequential FCN-based classification model with an encoder-decoder structure and incorporated spatial information for pixel-wise semantic segmentation of background, crops and weeds. The model learned plant arrangement information from image sequences representing a part of the crop row and fused the information with visual features, which improved the performance and generalization capabilities of the classification model.

4. Discussion and conclusion

This review summarized the current status of weed detection using ground-based machine vision and imaging processing techniques. Specifically, the four procedures, pre-processing, segmentation, feature extraction and classification, for weed detection were discussed in details. To separate vegetation from background, different color indices and classification approaches were applied and satisfactory results were obtained. The difficulty of weed detection lies in the discrimination between crops and weeds that often have similar properties. Generally, four categories of features, i.e., biological morphology, spectral features, visual textures and spatial contexts, were used for the task. These features were summarized in this review for quick reference, but these features are often mixed together to obtain promising results. The final classification procedure could be conducted using both conventional machine learning-based and recently developed deep learning-based approaches. There are commercialized products using machine vision and image processing techniques for weed detection and subsequent SSWM, such as the “Sense & Decide” from Blue River Technology (Sunnyvale, CA, U.S.), which was acquired by John Deere (Deere & Company, Miline, Illinois, U.S.), the autonomous weed robot by “ecoRobotix” (ecoRobotix Ltd, Switzerland) and “Deedfield Robotics” (Renningen, Baden-Wurttemberg, Germany), a young Bosch start-up. These intelligent products meet the demand of SSWM, and will surely open new market for weeding machines in the future.

Despite of the advances achieved in the past decade for weed detection, there still exist several challenges for real applications in the field, such as occlusion and overlap of leaves, varying lighting conditions and different growth stages, etc. Solutions on overcoming these challenges proposed by researchers were covered. These methods yielded good results for dedicated scenarios, but still lacked of generality and robustness. Deep learning-based approaches exhibit promising prospect, but large amount of labelled samples are necessary for training, which is labor-cost considering the retraining process for new applications. Therefore, new learning networks should be considered such as semi-supervised learning, self-taught learning, generative adversarial networks (GAN). To validate and compare the performance of newly developed algorithms, an image dataset with enough samples and corresponding ground truth annotations holds great significance. There are already datasets with images acquired on carrot (Haug and Ostermann, 2015) and sugar beet (Chebrolu et al., 2017) fields, as well an automatic model generated dataset for crop and weed detection (Cicco et al., 2016). These datasets are valuable for testing algorithms, but they only cover dedicated crops and weeds, and limited to specific growth stages, which should be extended further in the future. Another issue is the image processing time. Complicated algorithms generally provide better detection results, but with more processing time, limiting the weeding efficiency. A balance between accuracy and efficiency should be well considered.

Overall, machine vision with appropriate image processing algorithms is a very promising tool for precise real-time weed and crop detection in the field, which provides valuable sensing information for SSWM. Accurate crop detection is also beneficial to site-specific management of specialty crops, such as automatic harvest of cauliflower. Though there are still remaining challenges, the future is promising as there are many researchers concentrate their efforts on the task.

Acknowledgements

The authors gratefully acknowledge the financial support provided by the Natural Science Foundation of Jiangsu Province, China (No. BK20180861), and the Natural Science Foundation of the Jiangsu Higher Education Institutions of China (No. 14KJA210001).

Disclaimer of endorsement

Mention of commercial products, services, trade or brand names, organizations, or research studies in this publication does not imply endorsement by the authors, or Jiangsu University, nor discrimination against similar products, services, trade or brand names, organizations, or research studies not mentioned.

References

Ahmad, J., Muhammad, K., Ahmad, I., Ahmad, W., Smith, M.L., Smith, L.N., Jain, D.K., Wang, H., Mehmood, I., 2018. Visual features based boosted classification of weeds for real-time selective herbicide sprayer systems. Comput. Ind. 98, 23–33. https://doi.org/10.1016/j.compind.2018.02.005.

Ahmed, F., Al-Mamun, H.A., Bari, A.S.M.H., Hossain, E., Kwan, P., 2012. Classification of crops and weeds from digital images: a support vector machine approach. Crop Prot. 40, 98–104.

Akbarzadeh, S., Paap, A., Ahderom, S., Apopei, B., Alameh, K., 2018. Plant discrimination by Support Vector Machine classifier based on spectral reflectance. Comput. Electron. Agric. 148, 250–258. https://doi.org/10.1016/J.COMPAG.2018.03.026.

AlSuwaidi, A., Veys, C., Hussey, M., Grieve, B., Yin, H., 2016. Hyperspectral selection based algorithm for plant classification. In: 2016 IEEE International Conference on Imaging Systems and Techniques (IST). IEEE, pp. 395–400. https://doi.org/10.1109/IST.2016.7738258.

Andaló, F.A., Miranda, P.A.V., Torres, R.da S., Falcão, A.X., 2010. Shape feature extraction and description based on tensor scale. Pattern Recognit. 43, 26–36. https://doi.org/10.1016/J.PATCOG.2009.06.012.

Andújar, D., Rueda-Ayala, V., Moreno, H., Rosell-Polo, J., Escolá, A., Valero, C., Gerhards, R., Fernández-Quintanilla, C., Dorado, J., Griepentrog, H.-W., 2013. Discriminating crop, weeds and soil surface with a terrestrial LIDAR sensor. Sensors 13, 14662–14675. https://doi.org/10.3390/s131114662.

Arica, N., Yarman Vural, F.T., 2003. BAS: a perceptual shape descriptor based on the beam angle statistics. Pattern Recognit. Lett. 24, 1627–1639. https://doi.org/10.1016/S0167-8655(03)00002-3.

Ashok Kumar, D., Prema, P., 2013. A Review on Crop and Weed Segmentation Based on Digital Images. Springer, New Delhi, pp. 279–291.

Aware, A.A., Joshi, K., 2015. Wavelet based crop detection and automatic spraying of herbicides. Int. J. Innov. Adv. Comput. Sci. 4, 2–7.

Bai, X., Cao, Z., Wang, Y., Yu, Z., Hu, Z., Zhang, X., Li, C., 2014. Vegetation segmentation robust to illumination variations based on clustering and morphology modelling. Biosyst. Eng. 125, 80–97. https://doi.org/10.1016/J.BIOSYSTEMSENG.2014.06.015.

Bakhshipour, A., Jafari, A., 2018. Evaluation of support vector machine and artificial

neural networks in weed detection using shape features. Comput. Electron. Agric. 145, 153–160. https://doi.org/10.1016/J.COMPAG.2017.12.032.
Bakhshipour, A., Jafari, A., Nassiri, S.M., Zare, D., 2017. Weed segmentation using texture features extracted from wavelet sub-images. Biosyst. Eng. 157, 1–12. https://doi.org/10.1016/J.BIOSYSTEMSENG.2017.02.002.
Behmann, J., Mahlein, A.K., Rumpf, T., Römer, C., Plümer, L., 2015. A review of advanced machine learning methods for the detection of biotic stress in precision crop protection. Agric. Precis. https://doi.org/10.1007/s11119-014-9372-7.
Berge, T.W., Aastveit, A.H., Fykse, H., 2008. Evaluation of an algorithm for automatic detection of broad-leaved weeds in spring cereals. Precis. Agric. 9, 391–405.
Bharati, M.H., Liu, J.J., MacGregor, J.F., 2004. Image texture analysis: methods and comparisons. Chemom. Intell. Lab. Syst. 72, 57–71. https://doi.org/10.1016/j.chemolab.2004.02.005.
Brown, R.B., Noble, S.D., 2005. Site-specific weed management: sensing requirements - what do we need to see? Weed Sci. 53, 252–258.
Burgos-Artizzu, X.P., Ribeiro, A., Guijarro, M., Pajares, G., 2011. Real-time image processing for crop/weed discrimination in maize fields. Comput. Electron. Agric. 75, 337–346.
Burgos-Artizzu, X.P., Ribeiro, A., Tellaeche, A., Pajares, G., Fernández-Quintanilla, C., 2009. Improving weed pressure assessment using digital images from an experience-based reasoning approach. Comput. Electron. Agric. 65, 176–185. https://doi.org/10.1016/j.compag.2008.09.001.
Campos, Y., Sossa, H., Pajares, G., 2017. Comparative analysis of texture descriptors in maize fields with plants, soil and object discrimination. Precis. Agric. 18, 717–735. https://doi.org/10.1007/s11119-016-9483-4.
Chaki, J., Parekh, R., Bhattacharya, S., 2015. Plant leaf recognition using texture and shape features with neural classifiers. Pattern Recognit. Lett. 58, 61–68. https://doi.org/10.1016/j.patrec.2015.02.010.
Che'Ya, N.N., 2016. Site-Specific Weed Management Using Remote Sensing. University of Queensland.
Chebrolu, N., Lottes, P., Schaefer, A., Winterhalter, W., Burgard, W., Stachniss, C., 2017. Agricultural robot dataset for plant classification, localization and mapping on sugar beet fields. Int. J. Rob. Res. 36, 1045–1052.
Cheng, B., Matson, E.T., 2015. A Feature-Based Machine Learning Agent for Automatic Rice and Weed Discrimination. Springer, Cham, pp. 517–527.
Cheng, H.D., Jiang, X.H., Sun, Y., Wang, J., 2001. Color image segmentation: advances and prospects. Pattern Recognit. 34, 2259–2281. https://doi.org/10.1016/S0031-3203(00)00149-7.
Chris Gliever, D.C.S., 2001. Crop verses Weed Recognition with Artificial Neural Networks, in: 2001 Sacramento, CA July 29-August 1,2001. American Society of Agricultural and Biological Engineers, St. Joseph, MI, p. 1. https://doi.org/10.13031/2013.7425.
Cicco, M. Di, Potena, C., Grisetti, G., Pretto, A., 2016. Automatic Model Based Dataset Generation for Fast and Accurate Crop and Weeds Detection. CoRR abs/1612.0, 5188–5195.
Cordill, C., Grift, T.E., 2011. Design and testing of an intra-row mechanical weeding machine for corn. Biosyst. Eng. 110, 247–252. https://doi.org/10.1016/J.BIOSYSTEMSENG.2011.07.007.
Dammer, K.-H., Intress, J., Beuche, H., Selbeck, J., Dworak, V., 2013. Discrimination of Ambrosia artemisiifolia and Artemisia vulgaris by hyperspectral image analysis during the growing season. Weed Res. 53, 146–156.
de Castro, A.-I., Jurado-Expósito, M., Gómez-Casero, M.-T., López-Granados, F., 2012. Applying neural networks to hyperspectral and multispectral field data for discrimination of cruciferous weeds in winter crops. Sci. World J. 2012, 1–11. https://doi.org/10.1100/2012/630390.
De Rainville, F.-M., Durand, A., Fortin, F.-A., Tanguy, K., Maldague, X., Panneton, B., Simard, M.-J., 2014. Bayesian classification and unsupervised learning for isolating weeds in row crops. Pattern Anal. Appl. 17, 401–414. https://doi.org/10.1007/s10044-012-0307-5.
Dyrmann, M., Jørgensen, R.N., Midtiby, H.S., 2017. RoboWeedSupport - Detection of weed locations in leaf occluded cereal crops using a fully convolutional neural network. Adv. Anim. Biosci. 8, 842–847. https://doi.org/10.1017/S2040470017000206.
Dyrmann, M., Karstoft, H., Midtiby, H.S., 2016. Plant species classification using deep convolutional neural network. Biosyst. Eng. 151, 72–80. https://doi.org/10.1016/J.BIOSYSTEMSENG.2016.08.024.
Fernández-Quintanilla, C., Peña, J.M., Andújar, D., Dorado, J., Ribeiro, A., López-Granados, F., 2018. Is the current state of the art of weed monitoring suitable for site-specific weed management in arable crops? Weed Res. 58, 259–272. https://doi.org/10.1111/wre.12307.
Frey, B.J., Drueck, D., 2006. Mixture modeling by affinity propagation. Adv. Neural Inf. Process. Syst. 18, 379–386.
García-Mateos, G., Hernández-Hernández, J.L., Escarabajal-Henarejos, D., Jaén-Terrones, S., Molina-Martínez, J.M., 2015. Study and comparison of color models for automatic image analysis in irrigation management applications. Agric. Water Manag. 151, 158–166. https://doi.org/10.1016/J.AGWAT.2014.08.010.
García-Santillán, I., Guerrero, J.M., Montalvo, M., Pajares, G., 2018. Curved and straight crop row detection by accumulation of green pixels from images in maize fields. Precis. Agric. 19, 18–41. https://doi.org/10.1007/s11119-016-9494-1.
García-Santillán, I.D., Montalvo, M., Guerrero, J.M., Pajares, G., 2017. Automatic detection of curved and straight crop rows from images in maize fields. Biosyst. Eng. 156, 61–79. https://doi.org/10.1016/J.BIOSYSTEMSENG.2017.01.013.
García-Santillán, I.D., Pajares, G., 2018. On-line crop/weed discrimination through the Mahalanobis distance from images in maize fields. Biosyst. Eng. 166, 28–43. https://doi.org/10.1016/J.BIOSYSTEMSENG.2017.11.003.
Gée, C., Bossu, J., Jones, G., Truchetet, F., 2008. Crop/weed discrimination in perspective agronomic images. Comput. Electron. Agric. 60, 49–59. https://doi.org/10.1016/J.COMPAG.2007.06.003.
Golzarian, M.R., Frick, R.A., 2011. Classification of images of wheat, ryegrass and brome grass species at early growth stages using principal component analysis. Plant Methods 7, 28. https://doi.org/10.1186/1746-4811-7-28.
Gonzalez, R.C., Woods, R.E., 2007. Image processing. Digit. image Process. 2.
Guerrero, J.M., Guijarro, M., Montalvo, M., Romeo, J., Emmi, L., Ribeiro, A., Pajares, G., 2013. Automatic expert system based on images for accuracy crop row detection in maize fields. Expert Syst. Appl. 40, 656–664. https://doi.org/10.1016/J.ESWA.2012.07.073.
Guerrero, J.M., Pajares, G., Montalvo, M., Romeo, J., Guijarro, M., 2012. Support Vector Machines for crop/weeds identification in maize fields. Expert Syst. Appl. 39, 11149–11155.
Guerrero, J.M., Ruz, J.J., Pajares, G., 2017. Crop rows and weeds detection in maize fields applying a computer vision system based on geometry. Comput. Electron. Agric. 142, 461–472. https://doi.org/10.1016/j.compag.2017.09.028.
Guijarro, M., Pajares, G., Riomoros, I., Herrera, P.J., Burgos-Artizzu, X.P., Ribeiro, A., 2011. Automatic segmentation of relevant textures in agricultural images. Comput. Electron. Agric. 75, 75–83. https://doi.org/10.1016/J.COMPAG.2010.09.013.
Guo, W., Rage, U.K., Ninomiya, S., 2013. Illumination invariant segmentation of vegetation for time series wheat images based on decision tree model. Comput. Electron. Agric. 96, 58–66.
Hague, T., Tillett, N.D., Wheeler, H., 2006. Automated crop and weed monitoring in widely spaced cereals. Precis. Agric. 7, 21–32. https://doi.org/10.1007/s11119-005-6787-1.
Hall, D., Dayoub, F., Kulk, J., McCool, C., 2017. Towards unsupervised weed scouting for agricultural robotics. In: Robotics and Automation (ICRA), 2017 IEEE International Conference On. IEEE, pp. 5223–5230.
Hall, D., McCool, C., Dayoub, F., Sunderhauf, N., Upcroft, B., 2015. Evaluation of Features for Leaf Classification in Challenging Conditions. In: 2015 IEEE Winter Conference on Applications of Computer Vision (WACV). IEEE, pp. 797–804.
Hamuda, E., Glavin, M., Jones, E., 2016. A survey of image processing techniques for plant extraction and segmentation in the field. Comput. Electron. Agric. 125, 184–199.
Hamuda, E., Mc Ginley, B., Glavin, M., Jones, E., 2018. Improved image processing-based crop detection using Kalman filtering and the Hungarian algorithm. Comput. Electron. Agric. 148, 37–44. https://doi.org/10.1016/j.compag.2018.02.027.
Hamuda, E., Mc Ginley, B., Glavin, M., Jones, E., 2017. Automatic crop detection under field conditions using the HSV colour space and morphological operations. Comput. Electron. Agric. 133, 97–107.
Hao, P., Wang, L., Niu, Z., 2015. Comparison of hybrid classifiers for crop classification using normalized difference vegetation index time series: a case study for major crops in North Xinjiang, China. PLoS One 10, e0137748–24.
Haralick, R.M., Shanmugam, K., Dinstein, I., 1973. Textural features for image classification. IEEE Trans. Syst. Man. Cybern. SMC-3, 610–621. https://doi.org/10.1109/TSMC.1973.4309314.
Hassanein, M., Lari, Z., El-Sheimy, N., Hassanein, M., Lari, Z., El-Sheimy, N., 2018. A new vegetation segmentation approach for cropped fields based on threshold detection from hue histograms. Sensors 18, 1253. https://doi.org/10.3390/s18041253.
Haug, S., Michaels, A., Biber, P., Ostermann, J., 2014. Plant classification system for crop /weed discrimination without segmentation. In: 2014 IEEE Winter Conference on Applications of Computer Vision (WACV). IEEE, pp. 1142–1149.
Haug, S., Ostermann, J., 2015. A Crop/Weed Field Image Dataset for the Evaluation of Computer Vision Based Precision Agriculture Tasks. Springer, Cham, pp. 105–116.
Hernández-Hernández, J.L., García-Mateos, G., González-Esquiva, J.M., Escarabajal-Henarejos, D., Ruiz-Canales, A., Molina-Martínez, J.M., 2016. Optimal color space selection method for plant/soil segmentation in agriculture. Comput. Electron. Agric. 122, 124–132. https://doi.org/10.1016/J.COMPAG.2016.01.020.
Herrera, P., Dorado, J., Ribeiro, A., 2014. A novel approach for weed type classification based on shape descriptors and a fuzzy decision-making method. Sensors 14, 15304–15324.
Herrmann, I., Shapira, U., Kinast, S., Karnieli, A., Bonfil, D.J., 2013. Ground-level hyperspectral imagery for detecting weeds in wheat fields. Precis. Agric. 14, 637–659.
Huang, Y., Lee, M.A., Thomson, S.J., Reddy, K.N., 2016. Ground-based hyperspectral remote sensing for weed management in crop production. Int. J. Agric. Biol. Eng. 9, 98–109.
Hunt, E.R., Cavigelli, M., Daughtry, C.S.T., Mcmurtrey, J.E., Walthall, C.L., 2005. Evaluation of digital photography from model aircraft for remote sensing of crop biomass and nitrogen status. Precis. Agric. 6, 359–378. https://doi.org/10.1007/s11119-005-2324-5.
Ishak, A.J., Hussain, A., Mustafa, M.M., 2009. Weed image classification using Gabor wavelet and gradient field distribution. Comput. Electron. Agric. 66, 53–61.
Jeon, H.Y., Tian, L.F., Zhu, H., 2011. Robust crop and weed segmentation under uncontrolled outdoor illumination. Sensors 11, 6270–6283. https://doi.org/10.3390/s110606270.
Ji, R., Qi, L., 2011. Crop-row detection algorithm based on Random Hough Transformation. Math. Comput. Model. 54, 1016–1020. https://doi.org/10.1016/j.mcm.2010.11.030.
Johnson, S.C., 1967. Hierarchical clustering schemes. Psychometrika 32, 241–254.
Jones, G., Gée, C., Truchetet, F., 2009. Assessment of an inter-row weed infestation rate on simulated agronomic images. Comput. Electron. Agric. 67, 43–50. https://doi.org/10.1016/J.COMPAG.2009.02.009.
Jurado-Expósito, M., López-Granados, F., Atenciano, S., García-Torres, L., González-Andújar, J.L., 2003. Discrimination of weed seedlings, wheat (Triticum aestivum) stubble and sunflower (Helianthus annuus) by near-infrared reflectance spectroscopy (NIRS). Crop Prot. 22, 1177–1180.

Kapur, J.N., Sahoo, P.K., Wong, A.K.C., 1985. A new method for gray-level picture thresholding using the entropy of the histogram. Comput. Vision Graph. Image Process. 29, 273–285. https://doi.org/10.1016/0734-189X(85)90125-2.
Kataoka, T., Kaneko, T., Okamoto, H., Hata, S., 2003. Crop growth estimation system using machine vision. In: Proceedings 2003 IEEE/ASME International Conference on Advanced Intelligent Mechatronics (AIM 2003). IEEE, pp. b1079–b1083. https://doi.org/10.1109/AIM.2003.1225492.
Kaur, D., Kaur, Y., 2014. Various image segmentation techniques: a review. Int. J. Comput. Sci. Mob. Comput. 3, 809–814 date accessed: 18/05/2016.
Kazmi, W., Garcia-Ruiz, F., Nielsen, J., Rasmussen, J., Andersen, H.J., 2015. Exploiting affine invariant regions and leaf edge shapes for weed detection. Comput. Electron. Agric. 118, 290–299. https://doi.org/10.1016/J.COMPAG.2015.08.023.
Kumar, D.A., Prema, P., 2016. A novel wrapping curvelet transformation based angular texture pattern (WCTATP) extraction method for weed identification. ICTACT J. Image Video Process. 6.
Lee, W.S., Alchanatis, V., Yang, C., Hirafuji, M., Moshou, D., Li, C., 2010. Sensing technologies for precision specialty crop production. Comput. Electron. Agric. 74, 2–33.
Li, N., Grift, T.E., Yuan, T., Zhang, C., Momin, M.A., Li, W., 2016. Image processing for crop/weed discrimination in fields with high weed pressure, in: 2016 ASABE International Meeting. American Society of Agricultural and Biological Engineers, pp. 1–11.
Li, P., He, D., Qiao, Y., Yang, C., 2013. An application of soft sets in weed identification, in: 2013 Kansas City, Missouri, July 21 - July 24, 2013. American Society of Agricultural and Biological Engineers, St. Joseph, MI, p. 1.
Lin, C., 2009. A support vector machine embedded weed identification system. University of Illinois at Urbana-Champaign.
Liu, Lee, S.H., Saunders, C., 2014. Development of a machine vision system for weed detection during both off-sean and in-season in broadacre no-tillage cropping lands. Am. J. Agric. Biol. Sci. 9, 174–193. https://doi.org/10.3844/ajabssp.2014.174.193.
Longchamps, L., Panneton, B., Samson, G., Leroux, G.D., Thériault, R., 2009. Discrimination of corn, grasses and dicot weeds by their UV-induced fluorescence spectral signature. Precis. Agric. 11, 181–197.
López-Granados, F., 2011. Weed detection for site-specific weed management: mapping and real-time approaches. Weed Res. 51, 1–11. https://doi.org/10.1111/j.1365-3180.2010.00829.x.
Lottes, P., Behley, J., Milioto, A., Stachniss, C., 2018. Fully Convolutional Networks with Sequential Information for Robust Crop and Weed Detection in Precision Farming. arXiv Prepr. arXiv1806.03412.
Lottes, P., Hoeferlin, M., Sander, S., Muter, M., Schulze, P., Stachniss, L.C., 2016. An effective classification system for separating sugar beets and weeds for precision farming applications. In: 2016 IEEE International Conference on Robotics and Automation (ICRA). IEEE, pp. 5157–5163.
Lottes, P., Hörferlin, M., Sander, S., Stachniss, C., 2016b. Effective vision-based classification for separating sugar beets and weeds for precision farming. J. F. Robot. 34, 1160–1178.
Materka, A., Strzelecki, M., 1998. Texture analysis methods – A review. Methods 11, 1–33doi:10.1.1.97.4968.
Mathanker, S.K., Weckler, P.R., Taylor, R.K., Fan, G., 2010. Adaboost and Support Vector Machine Classifiers for Automatic Weed Control: Canola and Wheat. In: 2010 Pittsburgh, Pennsylvania, June 20 - June 23, 2010. American Society of Agricultural and Biological Engineers, St. Joseph, MI, p. 1.
McCarthy, C., Rees, S., Baillie, C., 2010. Machine vision-based weed spot spraying: a review and where next for sugarcane?. In: Proceedings of the 32nd Annual Conference of the Australian Society of Sugar Cane Technologists (ASSCT 2010). Australian Society of Sugar Cane Technologists.
McCool, C., Perez, T., Upcroft, B., 2017. Mixtures of lightweight deep convolutional neural networks: applied to agricultural robotics. IEEE Robot. Autom. Lett. 2, 1344–1351.
Meyer, G.E., Camargo Neto, J., Jones, D.D., Hindman, T.W., 2004. Intensified fuzzy clusters for classifying plant, soil, and residue regions of interest from color images. Comput. Electron. Agric. 42, 161–180. https://doi.org/10.1016/J.COMPAG.2003.08.002.
Meyer, G.E., Hindman, T.W., Laksmi, K., 1999. Machine vision detection parameters for plant species identification. In: Meyer, G.E., DeShazer, J.A. (Eds.), International Society for Optics and Photonics, pp. 327–335 doi: 10.1117/12.336896.
Meyer, G.E., Neto, J.C., 2008. Verification of color vegetation indices for automated crop imaging applications. Comput. Electron. Agric. 63, 282–293.
Midtiby, H.S., Åstrand, B., Jørgensen, O., Jørgensen, R.N., 2016. Upper limit for context–based crop classification in robotic weeding applications. Biosyst. Eng. 146, 183–192. https://doi.org/10.1016/j.biosystemseng.2016.01.012.
Milioto, A., Lottes, P., Stachniss, C., 2018. Real-time Semantic Segmentation of Crop and Weed for Precision Agriculture Robots Leveraging Background Knowledge in CNNs. In: 2018 IEEE International Conference on Robotics and Automation (ICRA). pp. 2229–2235.
Ming-Kuei, Hu., 1962. Visual pattern recognition by moment invariants. IEEE Trans. Inf. Theory 8, 179–187. https://doi.org/10.1109/TIT.1962.1057692.
Montalvo, M., Pajares, G., Guerrero, J.M., Romeo, J., Guijarro, M., Ribeiro, A., Ruz, J.J., Cruz, J.M., 2012. Automatic detection of crop rows in maize fields with high weeds pressure. Expert Syst. Appl. 39, 11889–11897. https://doi.org/10.1016/j.eswa.2012.02.117.
Siddiqi, Muhammad Hameed, Seok-Won Lee, A.M.K., 2014. Weed image classification using wavelet transform, stepwise linear discriminant analysis and support vector machines for an automatic spray control system. J. Inf. Sci. Eng. 30, 1253–1270.
Mursalin, M., Mesbah-Ul-Awal, M., 2014. Towards Classification of Weeds through Digital Image. In: 2014 Fourth International Conference on Advanced Computing & Communication Technologies (ACCT). IEEE, pp. 1–4.
Nasrabadi, N.M., 2007. Pattern recognition and machine learning. J. Electron. Imag. 16, 49901.
Nørremark, M., Griepentrog, H.W., Nielsen, J., Søgaard, H.T., 2008. The development and assessment of the accuracy of an autonomous GPS-based system for intra-row mechanical weed control in row crops. Biosyst. Eng. 101, 396–410. https://doi.org/10.1016/J.BIOSYSTEMSENG.2008.09.007.
Otsu, N., 1979. A threshold selection method from gray-level histograms. IEEE Trans. Syst. Man. Cybern. 9, 62–66.
Pereira, L.A.M., Nakamura, R.Y.M., de Souza, G.F.S., Martins, D., Papa, J.P., 2012. Aquatic weed automatic classification using machine learning techniques. Comput. Electron. Agric. 87, 56–63.
Persson, M., Åstrand, B., 2008. Classification of crops and weeds extracted by active shape models. Biosyst. Eng. 100, 484–497. https://doi.org/10.1016/j.biosystemseng.2008.05.003.
Peteinatos, G.G., Weis, M., Andújar, D., Rueda Ayala, V., Gerhards, R., 2014. Potential use of ground-based sensor technologies for weed detection. Pest Manag. Sci. 70, 190–199. https://doi.org/10.1002/ps.3677.
Piron, A., Leemans, V., Kleynen, O., Lebeau, F., Destain, M.F., 2008. Selection of the most efficient wavelength bands for discriminating weeds from crop. Comput. Electron. Agric. 62, 141–148.
Piron, A., van der Heijden, F., Destain, M.F., 2010. Weed detection in 3D images. Precis. Agric. 12, 607–622.
Potena, C., Nardi, D., Pretto, A., 2017. Fast and Accurate Crop and Weed Identification with Summarized Train Sets for Precision Agriculture. In: Advances in Robot Design and Intelligent Control. Springer International Publishing, Cham, pp. 105–121.
Prema, P., Murugan, D., 2016. A Novel Angular Texture Pattern (ATP) extraction method for crop and weed discrimination using curvelet transformation. ELCVIA Electron. Lett. Comput. Vis. Image Anal. 15, 27–59.
Reiser, D., Martín-López, J., Memic, E., Vázquez-Arellano, M., Brandner, S., Griepentrog, H., 2017. 3D imaging with a sonar sensor and an automated 3-axes frame for selective spraying in controlled conditions. J. Imag. 3, 9. https://doi.org/10.3390/jimaging3010009.
Riegler-Nurscher, P., Prankl, J., Bauer, T., Strauss, P., Prankl, H., 2018. A machine learning approach for pixel wise classification of residue and vegetation cover under field conditions. Biosyst. Eng. 169, 188–198. https://doi.org/10.1016/j.biosystemseng.2018.02.011.
Rodrigo, M.A., Oturan, N., Oturan, M.A., 2014. Electrochemically assisted remediation of pesticides in soils and water: a review. Chem. Rev. 114, 8720–8745.
Romeo, J., Pajares, G., Montalvo, M., Guerrero, J.M., Guijarro, M., de la Cruz, J.M., 2013. A new Expert System for greenness identification in agricultural images. Expert Syst. Appl. 40, 2275–2286. https://doi.org/10.1016/J.ESWA.2012.10.033.
Romeo, J., Pajares, G., Montalvo, M., Guerrero, J.M., Guijarro, M., Ribeiro, A., 2012. Crop row detection in maize fields inspired on the human visual perception. Sci. World J. 2012, 1–10. https://doi.org/10.1100/2012/484390.
Ruiz-Ruiz, G., Gómez-Gil, J., Navas-Gracia, L.M., 2009. Testing different color spaces based on hue for the environmentally adaptive segmentation algorithm (EASA). Comput. Electron. Agric. 68, 88–96. https://doi.org/10.1016/J.COMPAG.2009.04.009.
Rumpf, T., Roemer, C., Weis, M., Soekefeld, M., Gerhards, R., Pluemer, L., 2012. Sequential support vector machine classification for small-grain weed species discrimination with special regard to Cirsium arvense and Galium aparine. Comput. Electron. Agric. 80, 89–96.
Saber, M., Lee, W.S., Burks, T.F., Schueller, J.K., Chase, C.A., MacDonald, G.E., Salvador, G.A., 2015. Performance and Evaluation of Intra-Row Weeder Ultrasonic Plant Detection System and Pinch-Roller Weeding Mechanism for Vegetable Crops. In: 2015 ASABE International Meeting. American Society of Agricultural and Biological Engineers, p. 1. https://doi.org/10.13031/aim.20152188868.
Sabzi, S., Abbaspour-Gilandeh, Y., García-Mateos, G., 2018. A fast and accurate expert system for weed identification in potato crops using metaheuristic algorithms. Comput. Ind. 98, 80–89. https://doi.org/10.1016/j.compind.2018.03.001.
Saeedeh Taghadomi-Saberi, A.H., 2015. Improving field management by machine vision - a review. In: Agricultural Engineering International: CIGR Journal. International Commission of Agricultural Engineering.
Saha, D., Hanson, A., Shin, S.Y., 2016. Development of Enhanced Weed Detection System with Adaptive Thresholding and Support Vector Machine, in: The International Conference. ACM Press, New York, New York, USA, pp. 85–88.
Shaner, D.L., Beckie, H.J., 2014. The future for weed control and technology. Pest Manag. Sci. 70, 1329–1339. https://doi.org/10.1002/ps.3706.
Shapira, U., Herrmann, I., Karnieli, A., Bonfil, D.J., 2013. Field spectroscopy for weed detection in wheat and chickpea fields. Int. J. Remote Sens. 34, 6094–6108. https://doi.org/10.1080/01431161.2013.793860.
Singh, A., Ganapathysubramanian, B., Singh, A.K., Sarkar, S., 2016. Machine learning for high-throughput stress phenotyping in plants. Trends Plant Sci. https://doi.org/10.1016/j.tplants.2015.10.015.
Slaughter, D.C., 2013. The Biological Engineer: Sensing the Difference Between Crops and Weeds. In: Automation: The Future of Weed Control in Cropping Systems. Springer, Netherlands, Dordrecht, pp. 71–95.
Slaughter, D.C., Giles, D.K., Downey, D., 2008. Autonomous robotic weed control systems: a review. Comput. Electron. Agric. 61, 63–78. https://doi.org/10.1016/j.compag.2007.05.008.
Søgaard, H.T., 2005. Weed classification by active shape models. Biosyst. Eng. 91, 271–281. https://doi.org/10.1016/J.BIOSYSTEMSENG.2005.04.011.
Sujaritha, M., Annadurai, S., Satheeshkumar, J., Kowshik Sharan, S., Mahesh, L., 2017. Weed detecting robot in sugarcane fields using fuzzy real time classifier. Comput. Electron. Agric. 134, 160–171.
Tang, J., Chen, X.-Q., Miao, R.-H., Wang, D., 2016. Weed detection using image

processing under different illumination for site-specific areas spraying. Comput. Electron. Agric. 122, 103–111.
Tang, J., Wang, D., Zhang, Z., He, L., Xin, J., Xu, Y., 2017. Weed identification based on K-means feature learning combined with convolutional neural network. Comput. Electron. Agric. 135, 63–70. https://doi.org/10.1016/J.COMPAG.2017.01.001.
Tang, J., Zhang, Z., Wang, D., Xin, J., He, L., 2018. Research on weeds identification based on K-means feature learning. Soft Comput. 1–10. https://doi.org/10.1007/s00500-018-3125-x.
Tannouche, A., Sbai, K., Rahmoune, M., Zoubir, A., Agounoune, R., Saadani, R., Rahmani, A., 2016. A fast and efficient shape descriptor for an advanced weed type classification approach. Int. J. Electr. Comput. Eng. 6, 1168–1175. https://doi.org/10.11591/ijece.v6i3.9978.
Tellaeche, A., Pajares, G., Burgos-Artizzu, X.P., Ribeiro, A., 2011. A computer vision approach for weeds identification through Support Vector Machines. Appl. Soft Comput. 11, 908–915.
Tian, L.F., Slaughter, D.C., 1998. Environmentally adaptive segmentation algorithm for outdoor image segmentation. Comput. Electron. Agric. 21, 153–168. https://doi.org/10.1016/S0168-1699(98)00037-4.
Tillett, N.D., Hague, T., Grundy, A.C., Dedousis, A.P., 2008. Mechanical within-row weed control for transplanted crops using computer vision. Biosyst. Eng. 99, 171–178. https://doi.org/10.1016/J.BIOSYSTEMSENG.2007.09.026.
Tremblay, N., Wang, Z., Ma, B.-L., Belec, C., Vigneault, P., 2009. A comparison of crop data measured by two commercial sensors for variable-rate nitrogen application. Precis. Agric. 10, 145–161. https://doi.org/10.1007/s11119-008-9080-2.
Tu, C., van Wyk, B.J., Djouani, K., Hamam, Y., Du, S., 2014. An efficient crop row detection method for agriculture robots. In: 2014 7th International Congress on Image and Signal Processing (CISP). IEEE, pp. 655–659.
van Gerven, M., Bohte, S., 2018. Artificial neural networks as models of neural information processing. Frontiers Media SA.
Vidović, I., Cupec, R., Hocenski, Ž., 2016. Crop row detection by global energy minimization. Pattern Recognit. 55, 68–86. https://doi.org/10.1016/J.PATCOG.2016.01.013.
Weis, M., Sökefeld, M., 2010. Detection and Identification of Weeds. In: Precision Crop Protection - the Challenge and Use of Heterogeneity. Springer, Netherlands, Dordrecht, pp. 119–134.
Woebbecke, D.M., Meyer, G.E., Bargen, K. Von, Mortensen, D.A., 1995. Color indices for weed identification under various soil, residue, and lighting conditions. Trans. ASAE 38, 259–269. https://doi.org/10.13031/2013.27838.
Woebbecke, D.M., Meyer, G.E., Von Bargen, K., Mortensen, D.A., 1993. Plant Species Identification, Size, and Enumeration Using Machine Vision Techniques on Near-Binary Images. In: DeShazer, J.A., Meyer, G.E. (Eds.), International Society for Optics and Photonics, pp. 208–219. https://doi.org/10.1117/12.144030.
Wu, L., Wen, Y., 2009. Weed/corn seedling recognition by support vector machine using texture features. African J. Agric. Res. 4, 840–846. https://doi.org/10.5897/AJAR.
Wu, X., Xu, W., Song, Y., Cai, M., 2011. A detection method of weed in wheat field on machine vision. Procedia Eng. 15, 1998–2003. https://doi.org/10.1016/J.PROENG.2011.08.373.
Yang, W., Wang, S., Zhao, X., Zhang, J., Feng, J., 2015. Greenness identification based on HSV decision tree. Inf. Process. Agric. 2. https://doi.org/10.1016/j.inpa.2015.07.003.
Yong Chen, Xiaojun Jin, Lie Tang, Jun Che, Yanxia Sun, Jun Chen, 2013. Intra-row weed recognition using plant spacing information in stereo images. In: 2013 Kansas City, Missouri, July 21 - July 24, 2013. American Society of Agricultural and Biological Engineers, St. Joseph, MI, p. 1. https://doi.org/10.13031/aim.20131592292.
Yu, Z., Li, C., Shi, G., 2018. Environmentally adaptive crop extraction for agricultural automation using super-pixel and LAB Gaussian model. In: Cao, Z., Wang, Y., Cai, C. (Eds.), MIPPR 2017: Pattern Recognition and Computer Vision. SPIE, pp. 63. https://doi.org/10.1117/12.2285490.
Zhang, J., Tan, T., 2002. Brief review of invariant texture analysis methods. Pattern Recognit. 35, 735–747. https://doi.org/10.1016/S0031-3203(01)00074-7.
Zheng, L., Shi, D., Zhang, J., 2010. Segmentation of green vegetation of crop canopy images based on mean shift and Fisher linear discriminant. Pattern Recognit. Lett. 31, 920–925. https://doi.org/10.1016/J.PATREC.2010.01.016.
Zheng, L., Zhang, J., Wang, Q., 2009. Mean-shift-based color segmentation of images containing green vegetation. Comput. Electron. Agric. 65, 93–98. https://doi.org/10.1016/J.COMPAG.2008.08.002.
Zwiggelaar, R., 1998. A review of spectral properties of plants and their potential use for crop/weed discrimination in row-crops. Crop Prot. 17, 189–206.